

**IASI carbon
monoxide validation
over the Arctic during
POLARCAT**

M. Pommier et al.

IASI carbon monoxide validation over the Arctic during POLARCAT spring and summer campaigns

M. Pommier¹, K. S. Law¹, C. Clerbaux^{1,3}, S. Turquety², D. Hurtmans³,
J. Hadji-Lazaro¹, P.-F. Coheur³, H. Schlager⁴, G. Ancellet¹, J.-D. Paris⁵,
P. Nédélec⁶, G. S. Diskin⁷, J. R. Podolske⁸, J. S. Holloway^{9,10}, and P. Bernath^{11,12}

¹UPMC Univ. Paris 06; Université Versailles St-Quentin; CNRS/INSU, UMR 8190, LATMOS-IPSL, Paris, France

²UPMC Univ. Paris 06; Ecole Polytechnique; CNRS UMR 8539, LMD-IPSL, Palaiseau, France

³Spectroscopie de l'Atmosphère, Chimie Quantique et Photophysique, Université Libre de Bruxelles (ULB), Brussels, Belgium

⁴DLR, Institut für Physik der Atmosphäre, Oberpfaffenhofen, Germany

⁵LSCE/IPSL, CEA-CNRS-UVSQ, Saclay, France

Title Page

Abstract

Introduction

Conclusions

References

Tables

Figures

⏪

⏩

◀

▶

Back

Close

Full Screen / Esc

Printer-friendly Version

Interactive Discussion

**IASI carbon
monoxide validation
over the Arctic during
POLARCAT**M. Pommier et al.

[Title Page](#)[Abstract](#)[Introduction](#)[Conclusions](#)[References](#)[Tables](#)[Figures](#)[⏪](#)[⏩](#)[◀](#)[▶](#)[Back](#)[Close](#)[Full Screen / Esc](#)[Printer-friendly Version](#)[Interactive Discussion](#)

⁶Université de Toulouse, UPS, LA (Laboratoire d'Aérodynamique), CNRS UMR 5560, Toulouse, France

⁷NASA Langley Research Center, MS 483, Hampton, USA

⁸NASA Ames Research Center, Moffett Field, California, 94035, USA

⁹Chemical Sciences Division, NOAA Earth System Research Laboratory, Boulder, Colorado, USA

¹⁰Cooperative Institute for Research in Environmental Sciences, University of Colorado, Boulder, Colorado, USA

¹¹Department of Chemistry, University of Waterloo, Waterloo, Ontario, N2L 3G1, Canada

¹²Department of Chemistry, University of York, Heslington, York, YO10 5DD, UK

Received: 22 April 2010 – Accepted: 7 May 2010 – Published: 9 June 2010

Correspondence to: M. Pommier (matthieu.pommier@latmos.ipsl.fr)

Published by Copernicus Publications on behalf of the European Geosciences Union.

Abstract

In this paper, we provide a detailed comparison between carbon monoxide (CO) data measured by the Infrared Atmospheric Sounding Interferometer (IASI)/METOP and aircraft measurements over the Arctic. The CO measurements were obtained during North American campaigns (NASA ARCTAS and NOAA ARCPAC) and European campaigns (POLARCAT-France, POLARCAT-GRACE and YAK-AEROSIB) as part of the International Polar Year (IPY) in spring and summer 2008. During the campaigns different air masses were sampled including clean air, polluted plumes originating from anthropogenic sources in Europe, Asia and North America, and forest fire plumes originating from Siberia and Canada. CO-rich plumes following different transport pathways were captured well by the IASI instrument, illustrated for example by a transport event over the North Pole from Asia on 9 July 2008. The comparison between the IASI CO profiles and aircraft data was achieved by first completing the latter for higher altitudes using a latitudinally dependent climatology of ACE-FTS satellite CO profiles (2004–2009) and by subsequently smoothing the resulting full profiles by the IASI averaging kernels. Proceeding this way, the IASI profiles were shown to be in good agreement with smoothed in situ profiles (with a difference of about 10 ppbv) in spring. In summer, the IASI profiles were higher than the smoothed in situ profiles below 8 km, for all polluted cases. Correlations between IASI and combination ACE-FTS/aircraft derived total columns varied from 0.15 to 0.74 in spring and 0.26 to 0.84 in summer, with better results over the sea in spring (0.73) and over the land in summer (0.69).

1 Introduction

The Arctic atmosphere is a natural receptor of pollution from the continents of the Northern Hemisphere. The Arctic troposphere was believed to be extremely clean until the 1950s, when flights above the Canadian and Alaskan Arctic went through strong haze, decreasing the visibility (Greenaway, 1950; Mitchell, 1957). This so-called “Arctic

IASI carbon monoxide validation over the Arctic during POLARCAT

M. Pommier et al.

Title Page

Abstract

Introduction

Conclusions

References

Tables

Figures



Back

Close

Full Screen / Esc

Printer-friendly Version

Interactive Discussion



**IASI carbon
monoxide validation
over the Arctic during
POLARCAT**M. Pommier et al.

[Title Page](#)[Abstract](#)[Introduction](#)[Conclusions](#)[References](#)[Tables](#)[Figures](#)[⏪](#)[⏩](#)[◀](#)[▶](#)[Back](#)[Close](#)[Full Screen / Esc](#)[Printer-friendly Version](#)[Interactive Discussion](#)

Haze” is a recurring phenomenon that has been observed every winter and spring. The origin of this pollution is long-range transport of aerosols and accumulation of persistent pollutants such as mercury and ozone (O_3). Recent studies (e.g. Shindell et al., 2008; Stohl, 2006) show that the Arctic troposphere is influenced, according to the season, by emissions from Europe, North America or Asia. These pollutants originate from large urban areas, as well as from boreal fires. Atmospheric pollution in this region may be having an effect on human health and also on climate through direct radiative effects or indirect effects such as enhanced summer sea-ice melt resulting from deposition of black carbon aerosols on snow and ice (Law and Stohl, 2007). Tropospheric ozone, an important greenhouse gas, could contribute, according to model simulations, to about 0.4°C to 0.5°C of winter and spring Arctic warming (Shindell et al., 2006). In the free troposphere, limited measurements such as those at Summit, Greenland, show a late spring/early summer maximum (Helmig et al., 2007). Ozone can either be photochemically produced in mid-latitude source regions or during transport to the Arctic where transport from the upper troposphere or lower stratosphere is also a source. Carbon monoxide (CO) has been used in a number of studies as a tracer of pollution transport thanks to its relatively long lifetime of several weeks in the troposphere. In addition, CO is an important precursor of ozone through photochemical production, in the presence of nitrogen oxides (NO_x). It is mainly produced by the combustion of fossil fuels by industry, car traffic or domestic heating system, and vegetation combustion or forest fires (e.g. Badr and Probert, 1995). It is also produced in the atmosphere by oxidation of methane (CH_4) and non-methane hydrocarbons (NMHC) by hydroxyl radical (OH). Since its main sink is reaction with OH, CO has an important role in the oxidizing power of the atmosphere, regulating the concentrations of CH_4 and O_3 .

In recent decades many surface and in situ measurements have been made in the Arctic from ground stations, aircraft and balloon-borne platforms, providing observations of several trace species, including CO. Intensive field campaigns using airborne instrumentation often measure enough species to allow detailed analysis of the chemical composition of the air masses. Several past campaigns have sampled pollution

transport events such as the Arctic Boundary Layer Expedition (ABLE) in 1988 (Harriss et al., 1992), the Tropospheric Ozone Production about the Spring Equinox (TOPSE) in 2000 (Atlas et al., 2003) and the International Consortium for Atmospheric Research on Transport and Transformation (ICARTT) in 2004 (Fehsenfeld et al., 2006). More recently, several aircraft campaigns were conducted in 2008 in the framework of the International Polar Year (IPY), focusing on pollutant transport (trace gas and aerosol), climate and Arctic tropospheric chemistry studies as part of the International Global Atmospheric Chemistry (IGAC) activity POLARCAT (Polar Study using Aircraft, Remote Sensing, Surface Measurements and Models, of Climate, Chemistry, Aerosols, and Transport). Observations from these aircraft campaigns, which were collected over a period of several weeks, provide a snapshot of Arctic chemical composition. They are more spatially and temporally sparsely than satellite data which, even if their accuracy is lower, can provide global and continuous monitoring of the distributions of several trace gases, including CO. Satellite data have clearly shown long-range transport of CO plumes between continents (Turquety et al., 2007; Rinsland et al., 2007; McMillan et al., 2008; Yurganov et al., 2008; Fisher et al., 2010). The Infrared Atmospheric Sounding Interferometer (IASI) instrument, launched on board the polar-orbiting METOP-A satellite on 19 October 2006, is the first of three consecutive instruments to be launched on the METOP satellites. METOP-A has a sun-synchronous orbit with a 09:30 local equator crossing time. With 14 daily orbits and a large scanning swath of 2200 km across the track, IASI provides global Earth coverage twice a day, and is thus particularly well suited for the analysis of long-range transport. Moreover, its polar orbit (inclination of 98.7°) allows enhanced coverage above the polar regions. However, the nadir-viewing geometry implies limited vertical resolution, typically ~6 km for CO, with one to two independent pieces of information on the vertical distribution, depending mostly on surface temperature/thermal contrast (George et al., 2009; Clerbaux et al., 2009). Limb observations allow the retrieval of vertical profiles with improved vertical resolution, but do not allow measurements below the mid-upper troposphere (<6 km) and are limited in terms of spatial coverage compared to a nadir observation

**IASI carbon
monoxide validation
over the Arctic during
POLARCAT**M. Pommier et al.

[Title Page](#)[Abstract](#)[Introduction](#)[Conclusions](#)[References](#)[Tables](#)[Figures](#)[⏪](#)[⏩](#)[◀](#)[▶](#)[Back](#)[Close](#)[Full Screen / Esc](#)[Printer-friendly Version](#)[Interactive Discussion](#)

**IASI carbon
monoxide validation
over the Arctic during
POLARCAT**M. Pommier et al.

[Title Page](#)[Abstract](#)[Introduction](#)[Conclusions](#)[References](#)[Tables](#)[Figures](#)[⏪](#)[⏩](#)[◀](#)[▶](#)[Back](#)[Close](#)[Full Screen / Esc](#)[Printer-friendly Version](#)[Interactive Discussion](#)

instruments. For example, ACE-FTS (Fourier Transform Spectrometer), the main instrument of Atmospheric Chemistry Experiment (ACE) mission, launched on board the Canadian SCISAT-1 satellite on 12 August 2003 (Bernath et al., 2005), observes vertical profiles of numerous trace species using solar occultation measurement geometry.

5 Daily ACE-FTS CO measurements are obtained for up to fifteen sunrises and fifteen sunsets every 24 h (Clerbaux et al., 2008).

Satellite data need to be validated against independent measurements. The IASI CO retrievals have recently been evaluated through comparisons with other satellite-borne instrument data (MOPITT, TES and AIRS) (George et al., 2009), showing good performance compared to other thermal infrared remote sensors but as yet they had not been evaluated against in situ observations. In this paper, we evaluate the quality of the IASI CO data in the Arctic, taking advantage of the intensive aircraft campaigns undertaken in 2008. Many in situ CO profiles were collected during landing, take-off, pollution exploration and from specific satellite validation flights. Specific difficulties associated with retrievals above the Arctic are investigated such as retrievals over ice, satellite observations above source regions as well as the seasonal variation of CO observations. Since the airborne observations are only performed up to ~7–12 km (depending on the aircraft capabilities), the vertical profiles retrieved from the IASI nadir radiance measurements were compared with in situ profiles completed with a climatology we built with ACE-FTS CO profiles for different seasons and latitudes.

The paper is organized as follows: after an overview of the aircraft campaigns and satellite observations (IASI and ACE-FTS) used in this paper (Sects. 2 and 3), the general meteorological conditions during spring and summer campaigns are presented (Sect. 4.1). IASI CO observations in the Arctic and the possibility of tracking long-range CO transport events are discussed, based on a qualitative comparison between IASI and the aircraft measurements (Sect. 4.2 and 4.3). The methodology adopted to validate IASI CO is outlined in Sect. 5.1. It is then used to provide a quantitative comparison (Sect. 5.2) and statistical evaluation of the quality of the IASI CO retrievals in spring and summer 2008 (Sect. 5.3). Conclusions are presented in Sect. 6.

2 Objectives and sampling areas of the Arctic campaigns in 2008

As part of POLARCAT, several aircraft campaigns were carried out in spring and summer 2008. Each campaign had its own particular goals as well as the general goal of improving our knowledge about sources, transport pathways and climate impacts of Arctic pollution. Here, we provide brief details about these campaigns.

2.1 POLARCAT-France and POLARCAT-GRACE

The POLARCAT-France campaigns took place between 30 March and 14 April 2008, from Kiruna, northern Sweden, and between 30 June and 14 July 2008 from Kangerlussuaq on the western coast of Greenland. The main objectives of the POLARCAT-France spring campaign were to study the Arctic front, transport of European and Asian (Siberian) pollutants to the Arctic and aerosol-cloud interactions and their impact on aerosol radiative forcing (Adam De Villiers et al., 2009). On the other hand, the summer campaign was mainly dedicated to the study of boreal forest fires emissions and pollutants transport, and the determination of the impact of these emissions on the chemical composition of the Arctic troposphere. Aerosol properties, O₃, H₂O and CO were measured by the French ATR-42 aircraft as well as O₃ and aerosol lidar measurements. During the spring and summer campaigns, specific IASI validation flights were performed. For these IASI validation flights, the ATR-42 made spirals during profiles. These profiles were made in the IASI scanning area close to satellite overpass time. At the same time (30 June to 18 July 2008) there was the German POLARCAT-GRACE (GREENland Aerosol and Chemistry Experiment) campaign using the DLR Falcon-20. The Falcon-20 measurements included O₃, CO, CO₂, H₂O, NO, NO₂, PAN, NO_y, $j(\text{NO}_2)$ and aerosol concentration and size.

During POLARCAT, flights sampled a range of different air masses: clean air, anthropogenic pollution from Europe and Asia (in spring), North America and Asia pollution (in summer), biomass burning plumes from Canada and Siberia, and often, a mixture of anthropogenic and forest fires plumes.

IASI carbon monoxide validation over the Arctic during POLARCAT

M. Pommier et al.

Title Page

Abstract

Introduction

Conclusions

References

Tables

Figures

⏪

⏩

◀

▶

Back

Close

Full Screen / Esc

Printer-friendly Version

Interactive Discussion



2.2 ARCPAC-ARCTAS

The Aerosol, Radiation, and Cloud Processes affecting Arctic Climate (ARCPAC) mission was conducted by NOAA (Warneke et al., 2009). This experiment was coordinated with the POLARCAT mission and the NOAA baseline climate research station at Barrow. The campaign lasted from 3 to 23 April 2008, based in Fairbanks, Alaska. Transit flights were on 3 and 23 April and research flights from Fairbanks took place from 11 to 21 April. The campaign investigated the chemical, optical and microphysical characteristics of aerosols and gas phase species in the Arctic springtime to determine the origin of sources (Warneke et al., 2009; Fisher et al., 2010). The instrumentation on board the aircraft was dedicated to CO, CO₂, H₂O, NO, NO₂, NO_y, PANs, SO₂, VOC and halogen measurements. Moreover, aerosol speciation (AMS), optical extinction, and black carbon measurements were also made, in addition to the microphysical properties.

Arctic Research of the Composition of the Troposphere from Aircraft and Satellites (ARCTAS) was directed by NASA (Jacob et al., 2009) with flight campaigns conducted in spring and summer 2008 as part of ARCTAS-A and ARCTAS-B with flights of the NASA DC-8 and P-3B. During the spring campaign based in Fairbanks, Alaska, flights focused on Arctic haze detection, aerosol radiative forcing and anthropogenic pollution studies, dovetailing the objectives of ARCPAC. The summer campaign, based in Cold Lake, Canada, focused on boreal forest fires and long-range transport impacts on the Arctic atmosphere. On board the DC-8 many measurements were performed including aerosol properties, black carbon (BC), SO₂, peroxy acetic acid, acetaldehyde, acetone, acetonitrile, benzene, isoprene, methanol, toluene, Hg, CO, O₃, CH₂O, H₂O₂, H₂O, HO₂, HCN, OH, HNO₃, PAN, NO, NO₂, NO_y, and H₂SO₄ (Jacob et al., 2009).

2.3 YAK-AEROSIB

As part of a joint French-Russian project, YAK-AEROSIB (Airborne Extensive Regional Observations in Siberia), flights were made in July 2008 with a Russian Antonov-30

IASI carbon monoxide validation over the Arctic during POLARCAT

M. Pommier et al.

Title Page

Abstract

Introduction

Conclusions

References

Tables

Figures



Back

Close

Full Screen / Esc

Printer-friendly Version

Interactive Discussion



over Siberia (Paris et al., 2009), and consisted of two large loops over northern and central Siberia. Flight routes, fixed six months before the campaign, were chosen with the aim of exploring different air mass origins. The most significant forest fire plumes were encountered on 11 July 2008 (Paris et al., 2009). Aerosol number, CO₂, CO, O₃, and H₂O were measured during the flights (Paris et al., 2008).

2.4 Summary of in situ observations used for IASI validation

All the flights used for comparison with the IASI CO retrievals are shown in Fig. 1, superimposed on the IASI monthly averaged total column CO map (1° × 1° grid) for April and July 2008. For both seasons, spring and summer, the validation was extended to all flights, using the transit flights and the flights from the ARCTAS-CARB (California Air Resources Board) deployment over California, described in Jacob et al. (2009), from 18 to 24 June 2008. According to the seasons and flight areas, different air masses were sampled, mainly in the free troposphere but sometimes in the boundary layer or lower stratosphere. These included clean air, polluted plumes originating from anthropogenic sources in Europe, Asia and North America, and forest fires plumes from Siberia and Canada. The IASI CO data used in this validation exercise were accumulated during both morning and afternoon orbits. Data collected were mainly in daytime as daylight is present during polar summer.

3 CO measurements

3.1 Satellite measurements

3.1.1 IASI

IASI is a high resolution nadir looking thermal infrared (IR) sounder. It is a Fourier Transform Spectrometer (FTS) that records radiance measurements from the Earth's surface and the atmosphere with a high spectral resolution of 0.5 cm⁻¹ (apodized)

IASI carbon monoxide validation over the Arctic during POLARCAT

M. Pommier et al.

Title Page

Abstract

Introduction

Conclusions

References

Tables

Figures

⏪

⏩

◀

▶

Back

Close

Full Screen / Esc

Printer-friendly Version

Interactive Discussion



IASI carbon monoxide validation over the Arctic during POLARCAT

M. Pommier et al.

Title Page

Abstract

Introduction

Conclusions

References

Tables

Figures

⏪

⏩

◀

▶

Back

Close

Full Screen / Esc

Printer-friendly Version

Interactive Discussion

a priori information was constructed using a database of CO profiles including aircraft profiles during landing and take-off from the MOZAIC (Measurements of OZone and water vapor by Airbus in-service airCRAFT) program (Nédélec et al., 2003), ACE-FTS satellite observations in the upper troposphere and lower stratosphere (Clerbaux et al., 2005) and distributions computed by the LMDz-INCA global chemistry-transport model (e.g. Turquety et al., 2008).

The FORLI-CO total column products were validated by George et al. (2009) through comparisons with other satellite retrievals. In the Northern Hemisphere, comparisons of IASI CO total columns with those of AIRS (Atmospheric InfraRed Sounders), MOPITT (Measurements Of Pollution in The Troposphere) and TES (Tropospheric Emission Spectrometer) have shown an agreement better than $\sim 7\%$. MOPITT is higher than IASI with an average bias of 11.4% for data north of 45° N. AIRS is in good agreement in the (45° ; 90° N) band (bias of 2.6% – correlation ~ 0.85) but in other regions discrepancies appear. AIRS CO data are larger than IASI for small concentrations ($\sim 11\%$) and lower for high concentrations ($\sim 17\%$). TES CO columns are globally lower than the IASI ones (6.2% for August 2008) (George et al., 2009). It was also evaluated in Turquety et al. (2009) for biomass burning plumes.

To characterize vertical sensitivity and resolution of IASI CO retrieval, the AK matrix and the Degree Of Freedom for Signal (DOFS) are used (Rodgers et al., 2000). DOFS represents the number of independent levels that can be retrieved and corresponds to the trace of AK matrix. The latter can be viewed as weighting function characterizing the vertical sensitivity of each CO measurement with the remainder of the information provided by the a priori profile. The study by George et al. (2009) also showed that IASI CO retrievals have between 0.8 and 2.4 pieces of independent vertical information. Below 1.0, this number shows profiles are contaminated by a priori contribution whereas above 1.0 the resolution of the profiles is better than a tropospheric column. Examples of IASI sensitivity are reported by George et al. (2009).

3.1.2 ACE-FTS

The SCISAT-1 satellite has a low Earth circular orbit (altitude 650 km, inclination 74°). On board, ACE-FTS, the main instrument of ACE mission, is a Fourier Transform Spectrometer measuring IR radiation in solar occultation mode. The mission allows the retrieval of a wide range of trace species due to the high signal to noise ratio of the measurements (Coheur et al., 2007). The instrument has a high spectral resolution (0.02 cm⁻¹) and measures the vertical distribution of trace gases, pressure and temperature typically from 10 to 100 km. Standard ACE-FTS products are volume mixing ratios of O₃, CH₄, H₂O, NO, NO₂, ClONO₂, HNO₃, N₂O, N₂O₅, HCl, CCl₃F, CCl₂F₂, HF and CO.

The CO profiles are retrieved by analysing occultation sequences (Boone et al., 2005; Clerbaux et al., 2005). This processing uses a global-fit method in a general non-linear least squares minimization scheme and a set of microwindows that vary with altitude in the fundamental 1-0 rotation-vibration band (around 4.7 μm) and in the overtone 2-0 band (2.3 μm). The intense 1-0 band provides information in the upper atmosphere and the 2-0 band at lowest altitudes when the signal from fundamental band saturates. In this paper, we use version 2.2 of CO operational retrievals for the spring and summer from 2004 to 2009, in order to build a climatology to complement the in situ measurements for the IASI CO validation.

3.2 In situ aircraft measurements

An overview of different CO measurements on board all the aircraft is listed in Table 1 including information about measurement precision and accuracy. The CO payload on the French ATR-42 used an IR absorption gas correlation with modified commercial gas analysers Thermo 48C and Thermo 49 (Thermo Environmental Instruments, USA) as in the MOZAIC program (Nédélec et al., 2003). Its accuracy has been improved by the addition of periodical zero measurements. The accuracy of these measurements is 5% (precision 5 ppbv) for 30 s integration time and the detection limit is 10 ppbv.

IASI carbon monoxide validation over the Arctic during POLARCAT

M. Pommier et al.

Title Page

Abstract

Introduction

Conclusions

References

Tables

Figures

⏪

⏩

◀

▶

Back

Close

Full Screen / Esc

Printer-friendly Version

Interactive Discussion



The instrument is calibrated with a CO standard referenced by NIST (National Institute of Standards and Technology) at $\pm 1\%$. A comparison with the DLR Falcon-20 data revealed a 7 ppbv negative difference between the ATR-42 and the Falcon-20. This was already noticed in previous studies (Ancellet et al., 2009) and related to differences in the calibration standard.

On board the German Falcon-20, the CO was measured with vacuum ultraviolet (UV) fluorescence technique using an AEROLASER instrument (Baehr et al., 2003). The precision and accuracy of the Falcon CO instrument is 2 ppbv and 5%, respectively.

The NOAA ARCPAC WP-3D aircraft which flew during spring 2008 used a vacuum UV fluorescence instrument to measure CO (Holloway et al., 2000).

Measurements of CO on the NASA DC-8 as part of ARCTAS were made using a tunable diode laser absorption (TDLAS) (Sachse et al., 1987) whilst measurements on the P-3B were made using the COBALT instrument, which employs off-axis Integrated Cavity Output Spectroscopy (oa-ICOS) (Provencal et al., 2005).

During YAK-AEROSIB, CO was also measured by similar instrumentation to that on the French ATR-42 using IR absorption gas correlation (Nédélec et al., 2003; Paris et al., 2008).

4 Analysis of IASI observations during Arctic campaigns

4.1 Long-range transport during the 2008 Arctic campaigns

A snapshot of the seasonal behaviour of CO is shown on Fig. 1. It highlights the seasonal cycle of CO, with higher concentrations in spring due to its longer lifetime and accumulation during the winter, as well as the main anthropogenic emission regions over Asia, North America and Europe and boreal fires in Siberia and Canada. Transport of CO downwind of continental regions can also be seen.

An example of the kind of measurements collected during spring is shown in Fig. 2 when as part of POLARCAT-France, measurements were made north of Scandinavia.

IASI carbon monoxide validation over the Arctic during POLARCAT

M. Pommier et al.

Title Page

Abstract

Introduction

Conclusions

References

Tables

Figures

⏪

⏩

◀

▶

Back

Close

Full Screen / Esc

Printer-friendly Version

Interactive Discussion



IASI carbon monoxide validation over the Arctic during POLARCAT

M. Pommier et al.

Title Page

Abstract

Introduction

Conclusions

References

Tables

Figures

⏪

⏩

◀

▶

Back

Close

Full Screen / Esc

Printer-friendly Version

Interactive Discussion



In this example, on 31 March 2008, IASI measurements show strong gradients over this region (Fig. 2b). They correspond to the position of the polar front, which blocked European pollution to the south (Fig. 2a). Note that since clouds were associated with the front and only clear-sky measurements are analysed with IASI, there is a lack of IASI observations over this area. Later, during April 2008, pollution was transported from agricultural fires in eastern Europe/western Russia, boreal fires in Siberia and from anthropogenic source regions in Asia across the high Arctic Ocean. Some of this pollution was transported to northern Scandinavia where it was observed by the ATR-42 (Adam de Villiers et al., 2009) and some across to Alaska and northern Canada (Warneke et al., 2009). Siberian burning plumes were transported to Alaska by cyclonic activity near Lake Baikal and over the northern Pacific (Fuelberg et al., 2010).

Summer meteorological conditions were different and, in general, weather systems were less intense during, for example, ARCTAS-B period compared to the spring (Fuelberg et al., 2010). During the aircraft campaigns based in western Greenland in July 2008, rather clean air masses were sampled at the beginning of the month. Then, a series of low-pressure systems have transported North American anthropogenic pollution and Canadian biomass burning plumes over southern Greenland. This was followed by air masses arriving from the north transporting pollution from Siberian boreal fires or Asia anthropogenic emission regions. The ARCTAS-B flights sampled Canadian boreal fire plumes (Jacob et al., 2009) whereas the YAK flights sampled Siberian fires (Paris et al., 2009). The daily coverage of IASI allows the detection of the CO long-range transport events. An example is illustrated in Fig. 3 which shows snapshots of four daily total column maps during July 2008. On 1 July 2008, CO source regions can be seen over Asia and North America. CO plumes from Asia were transported out of the continent and were divided into two branches on 5 July, one part crossing the North Pole and the second reaching the western coast of the US. By the 9 July, the Asian plume was transported directly over the Arctic to Greenland. North American plumes crossed the North Atlantic due to transport by frontal systems. On 11 July, these plumes can still be seen over Greenland although they were diluted due to mixing with

cleaner air masses. Also due to higher orography over Greenland, CO enhancements (plumes) are less evident. The supplement (<http://www.atmos-chem-phys-discuss.net/10/14445/2010/acpd-10-14445-2010-supplement.zip>) also highlights the different transport events from Asia and North America.

4.2 Performance of the IASI retrieval in Arctic

In the Arctic, the DOFS is lower than in the tropics due to the cold surface temperatures. Over the area relevant to this work (mid to high latitudes), as can be seen from Fig. 4, the DOFS ranges, in April, from 0.6 to 2.2 during the day and from 0.3 to 2.0 during the night. Daytime corresponds to a solar zenith angle (SZA) lower or equal to 83° and night-time to a SZA higher or equal to 90° . In July, the DOFS ranges from 1.0 to 2.3 in daytime and from 0.9 to 2.2 in night-time conditions. It is worth noting that due to the orography, small DOFS values are found over Greenland in spring and Northern China close to Mongolia in summer.

Figure 5 shows a monthly averaged distribution of the root-mean-square (RMS) error of the differences between observed and fitted spectra, characterizing the uncertainty in the retrieval (see Turquety et al., 2009), as well as the associated mean difference (bias), which is expressed as a percentage of the total RMS for daytime in both seasons. The RMS includes the errors due to the radiometric noise, the forward model (radiative transfer), in particular due to uncertainties on the temperature and water vapour profiles, aerosol contamination (although is expected to be low in the CO spectral range), as well as uncertainties on the CO adjusted profile. High RMS values are observed over land, especially in summer due to a stronger signal. Large errors are associated with emissivity issues due to sand over deserts (Sahara, Nevada or Gobi desert). Note that in the Turquety et al. (2009) study, data with RMS higher than $3.5 \times 10^{-9} \text{ W}/(\text{cm}^2 \text{ cm}^{-1} \text{ sr})$ were filtered out. Such high RMS values are not encountered in the Arctic region, from 1.19 to $1.40 \times 10^{-9} \text{ W}/(\text{cm}^2 \text{ cm}^{-1} \text{ sr})$ in April and from 1.45 to $1.70 \times 10^{-9} \text{ W}/(\text{cm}^2 \text{ cm}^{-1} \text{ sr})$ in July, north of 45° N , during the day (interquartile range). Table 2 summarizes the IASI performance over three northern source

IASI carbon monoxide validation over the Arctic during POLARCAT

M. Pommier et al.

Title Page

Abstract

Introduction

Conclusions

References

Tables

Figures

⏪

⏩

◀

▶

Back

Close

Full Screen / Esc

Printer-friendly Version

Interactive Discussion



emissions regions impacting the Arctic (North America, Asia, Europe), and two receptors regions (Pacific Ocean and North Pole) for both daytime and night-time conditions. Over each region, polluted conditions, where the CO total columns are higher or equal to 3×10^{18} molecules/cm² and the background conditions, where the total columns are lower than 3×10^{18} molecules/cm² were separated. Then the mean and standard deviation values were calculated. The overall RMS is around 1.5×10^{-9} W/(cm² cm⁻¹ sr) during the day and the night in April, with less than 14% due to the bias and around 1.8×10^{-9} W/(cm² cm⁻¹ sr) in July with less than 11% due to the bias. In each case, the RMS and the part due to the bias are higher for polluted conditions than for the background.

4.3 IASI CO vertical distribution: qualitative comparison with aircraft measurements

In this section, we discuss the consistency between IASI and the aircraft observations using direct comparisons, i.e. without accounting for the IASI limited vertical sensitivity. This qualitative approach allows evaluation of the IASI sensitivity to different plumes depending on the altitude and intensity of the events. A quantitative analysis follows in the next section.

4.3.1 Collocation criteria

In order to compare satellite observations and aircraft measurements, the first step is to check the place and time coincidence. Different coincidence criteria around the flight position were tested and here, comparisons were conducted using a stringent collocation criteria, i.e. a box of $0.2^\circ \times 0.2^\circ$ and time of ± 1 h. According to these criteria, the number of collocations per flight varies from 40 to 162 in spring and from 27 to 128 for the summer campaigns. This number also depends on the area covered by the aircraft, the duration of the flights and the cloud cover in the sampling area. The largest number of coincidences is obtained for the American flights during the spring campaigns, due

IASI carbon monoxide validation over the Arctic during POLARCAT

M. Pommier et al.

Title Page

Abstract

Introduction

Conclusions

References

Tables

Figures

⏪

⏩

◀

▶

Back

Close

Full Screen / Esc

Printer-friendly Version

Interactive Discussion



to their polar exploration and the good coverage of the METOP polar orbit at these high latitudes.

4.3.2 Analysis of IASI information along selected flights

Figure 6 shows three examples of CO distributions observed by the aircraft during spring flights of the ATR-42, the DC-8 and the WP-3D, along with the corresponding IASI retrievals. The number of IASI collocation is 162, 29 and 44, respectively. During these 3 flights, IASI is able to detect CO plumes to some extent. On 9 April, the DC-8 flew across the North Pole from Iqaluit (Eastern coast of Canada) to Fairbanks (Alaska). IASI detects the enhancement of European pollution at the end of the flight (“plume a”) above the land at 0–2 km. However, the retrieved concentrations remain lower than the in situ measurement by ~40 ppbv (parts per billion by volume). The main part of the flight was above the sea ice or above the snow and most of the IASI CO data have a DOFS around 1.0 with a lack of sensitivity at low altitude. On 10 April, IASI observed the same structure (~160 ppbv measured by in situ) above the Arctic Ocean close to the surface between 11:40 UTC and 12:30 UTC. Over this area, the sea is not frozen and the DOFS is around 1.10. Note that IASI did not detect the signature of CO in the first hour of the ATR-42 flight but snow was covering the land area and it might explain the lack of vertical sensitivity. On 18 April, the WP-3D sampled a Kazakhstan agricultural fire plume, aged 7–9 days, and a forest fire plume from Lake Baikal, aged about 4–5 days, identified on the plot as “plume a” and “plume b”. These plumes are described in detail by Warneke et al. (2009). IASI appears to observe a signature of agricultural fires around 4 km (“plume a”), of about 215 ppbv, compared to 223 ppbv observed by the NOAA aircraft (maximum around 250 ppbv). IASI did not observe a forest fire signature during the ascent and the descent around 23:00 UTC (“plume b”), due to the lack of sensitivity (DOFS~1.0) above the frozen sea in this season (described subsequently in Fig. 9c).

Similarly to Fig. 6, Fig. 7 shows three examples of summer flights which sampled Canadian forest fire plumes, a mixture of North American fires and anthropogenic

IASI carbon monoxide validation over the Arctic during POLARCAT

M. Pommier et al.

Title Page

Abstract

Introduction

Conclusions

References

Tables

Figures

⏪

⏩

◀

▶

Back

Close

Full Screen / Esc

Printer-friendly Version

Interactive Discussion



**IASI carbon
monoxide validation
over the Arctic during
POLARCAT**M. Pommier et al.

[Title Page](#)[Abstract](#)[Introduction](#)[Conclusions](#)[References](#)[Tables](#)[Figures](#)[⏪](#)[⏩](#)[◀](#)[▶](#)[Back](#)[Close](#)[Full Screen / Esc](#)[Printer-friendly Version](#)[Interactive Discussion](#)

plumes, and Siberian forest fire plumes with flights of the P-3B on 2 July, the Falcon-20 on 7 July and the Antonov-30 on 11 July 2008, respectively. The performance of IASI in detecting different events is illustrated by these examples. Along the P-3B flight on 2 July close to Canadian boreal fires, relatively good agreement is found between IASI and in situ CO measurements in the boundary layer with large CO signatures at 17:00 UTC and 18.30 UTC, labelled “plume a” and “plume b”, respectively. This is despite the fact that only 23 IASI pixels were found in the flight area. For both plumes, the maximum CO measured by the aircraft was around 1 ppmv while IASI observed around 700 ppbv in “plume a” and 450 ppbv in “plume b”. Here the IASI DOFS are around 1.5 and the maximum of sensitivity is between 2 and 7 km (not shown). During this flight, the NASA P-3B flew directly inside boreal forest fire plumes that were also detected by IASI in the south-eastern part of the flight. Two plumes, located from around 0.5 to 1.2 km, and from 0.6 to 1.8 km, respectively, were observed by IASI below 4 km. Background concentrations were also reasonably well observed after 18:00 UTC. On 7 July, the Falcon-20 flew in a mixture of North American forest fire and anthropogenic plumes in southern Greenland. 58 IASI collocations were found with a mean DOFS at 1.40. The in situ CO was around 160 ppbv and IASI CO about 120 ppbv. The DLR Falcon-20 measured a more extensive plume (in latitude) than IASI. On 11 July over Siberia, forest fires plumes were sampled by the Antonov-30 during the landing (“plume c”), described in Paris et al. (2009), and which was well captured by IASI with a DOFS around 1.7 (see Fig. 9d). This plume was encountered at low altitude, throughout the boundary layer very close to the source region (forest fires). IASI detected a signature around 350 ppbv when more than 600 ppbv was measured by the aircraft. Two other CO plumes in this flight (“plume a” and “plume b”) were not detected by IASI. These plumes were probably too thin for the satellite instrument vertical sensitivity to be detected. Concentrations in clean background air were also well captured by IASI during the rest of the flight. As obvious from Figs. 6 and 7, in summer, IASI achieves better vertical sensitivity, due to a higher thermal contrast, than in the springtime, resulting in improved detection of CO plumes during these hotter months.

5 Quantitative comparison between IASI and in situ profiles

5.1 Methodology

While cross-sections allow the observation of vertical structures, a quantitative comparison requires a specific consideration of instrumental and retrieval characteristics.

5 For a proper comparison of satellite data with in situ measurements, the AK information for each observation needs to be taken into account (Rodgers and Connor, 2003). The retrieved profile is obtained as follows,

$$\mathbf{x}_{\text{retrieved}} = \mathbf{A}_{\text{low}} \mathbf{x}_{\text{high}} + (\mathbf{I} - \mathbf{A}_{\text{low}}) \mathbf{x}_{\text{a,low}} \quad (1)$$

where \mathbf{A}_{low} represents the AK matrix characterizing the low resolution profiles, \mathbf{x}_{high} the true profile and $\mathbf{x}_{\text{a,low}}$ the a priori profile. In situ measurements were convolved with the IASI AK using Eq. (1). The aircraft profiles used in this validation exercise were recorded during either specific validation flights, like ATR-42 on 3 April 2008, or during take-off, landing or during deep vertical profiles in any flight. The IASI AK was applied to each in situ CO vertical profile in order to smooth the better resolved profile before comparison with co-located IASI data. Since most co-located ($\pm 0.2^\circ$; ± 1 h) aircraft profiles were limited in altitude (compared to the full satellite profile), the in situ profiles were extended using CO profiles retrieved from the ACE-FTS instrument in the upper troposphere and above. All available ACE-FTS profiles from 2004 to 2009 were used to compile seasonally averaged profiles for 15 degrees bins up to 60 km (same maximum altitude as IASI profiles). We used ACE-FTS data representative of each season, February to May for spring, and June to September for summer. Only profiles where there was no gap between the aircraft maximum altitude and the ACE-FTS minimum altitude were used in the validation procedure. The maximum altitudes reached by the different aircraft were 7 km for ATR-42 and WP-3D, 8 km for Antonov-30 and P-3B, 11 km for the Falcon-20 and 12 km for DC-8, respectively. Between 7 and 12 km this climatology shows a good coherence with sample of flights in this altitude range. Figure 8 shows an example of an in situ profile convolved with the IASI AK, and

14463

ACPD

10, 14445–14494, 2010

IASI carbon monoxide validation over the Arctic during POLARCAT

M. Pommier et al.

Title Page

Abstract

Introduction

Conclusions

References

Tables

Figures

⏪

⏩

◀

▶

Back

Close

Full Screen / Esc

Printer-friendly Version

Interactive Discussion



IASI carbon monoxide validation over the Arctic during POLARCAT

M. Pommier et al.

Title Page

Abstract

Introduction

Conclusions

References

Tables

Figures

⏪

⏩

◀

▶

Back

Close

Full Screen / Esc

Printer-friendly Version

Interactive Discussion



of a reconstructed profile obtained by combining in situ and ACE-FTS measurements, convolved with the IASI AK. This observation was made during the ATR-42 flight on 3 April 2008 during a validation profile above the sea at 71° N and 22° E. For this case the DOFS is ~ 1.15 , with a maximum sensitivity between 1 to 8 km and therefore measurement is best represented by a tropospheric column. It can be seen that when combined with the ACE-FTS climatology, the smoothed in situ profile is closer to the retrieved values from IASI. In the following we will refer to aircraft profiles completed using the ACE-FTS climatology (and convolved with IASI AK) as “smoothed in situ profiles”.

In the analysis that follows, we compared the smoothed in situ and IASI measurements both in terms of mixing ratio profiles and total columns (sum of partial columns).

5.2 Results: comparison of selected representative profiles

A systematic comparison was performed for all flights. Figure 9 shows three examples of comparisons in spring and three examples in summer highlighting different sampling conditions.

Figure 9a presents a CO profile above the Chukchi Sea, close to the Alaskan coast, in 9 April. The sea was frozen at this time and IASI did not distinguish the CO variability and the high signature around 5–6 km (~ 185 ppbv) as mentioned in Sect. 4.3.2. Nevertheless, after accounting for the limited IASI sensitivity, the agreement between smoothed in situ and IASI is good with a maximum difference between both profiles of 2.3 ppbv at 0.5 km in the in situ part (below 8.5 km), and of 6.4 ppbv at 12.5 km, where the ACE-FTS climatology was used.

The profile observed above Hudson Bay plotted in Figure 9b on 5 July shows that the DC-8 measured high CO concentrations between 5–8 km. IASI was not able to locate precisely this signature, but still captured an enhancement between 4 and 14 km in altitude. The smoothed in situ profile clearly highlights the lack of vertical resolution of the instrument, resulting in a broad enhancement in the mid-troposphere. Although IASI locates the plume in the correct altitude range, it strongly overestimates the CO

concentration compared to the in situ smoothed profile. IASI maximum mixing ratio is found at 10 km, compared to 6 km for the in situ profile. The profile before convolution was closer. We tested that when using higher values for the climatology in the UTLS (Upper Troposphere Lower Stratosphere), the smoothed in situ profile becomes closer to the IASI profile suggesting that there could have been enhanced CO concentrations at this time. Also note that the presence of sea ice in this area in spite of the season (see data from <http://www.ncdc.noaa.gov/snow-and-ice/>), could explain the problem of retrieval with the limited vertical sensitivity.

In cases (c) and (d) the two aircraft measured a Siberian biomass burning plume. As mentioned in Sect. 4.3.2 and illustrated on Fig. 6, the WP-3D measured an aged plume (Fig. 9c). Figure 9d shows the profile above the emission source during the landing of the Antonov-30 already shown in Fig. 7. For both examples, the retrieval fully smooths out the CO enhancements observed between 2–4 km and 6–7 km for the WP-3D and at 1 km and 3 km for the Antonov-30. This smoothing is clearly due to the lack of vertical sensitivity, with a DOFS~1.0 with the WP-3D and a limited sensitivity for the levels below 3 km seen with the Antonov-30. But the agreement between the IASI and the smoothed in situ profiles is good for the spring case. In summer, with the Antonov-30, a difference from 17 to 113 ppbv below 4.5 km is found between both profiles. Above 7 km, the difference is similar (10 ppbv) due to the ACE-FTS climatology.

Case (e) was measured during the take-off of the ATR-42 in Sweden on 31 March. IASI had problems detecting high CO signatures measured by the aircraft from the surface to 6 km probably due to the snow covering the land area and low thermal contrast (see the AK plot). Another explanation could be the collocation. Only one IASI collocated pixel was found, almost 50 min before the take-off and start of operation of the instruments so it is likely that IASI missed this plume, stretching the limits of collocation criteria. The difference between the smoothed in situ and IASI values is around 50 to 60 ppbv in the altitude range of the plume. Case (f) was also measured during a take-off of the ATR-42 but in Greenland on 10 July. Both IASI and the aircraft observed clean air with 8 IASI pixels found at almost the same time as the take-off. The

IASI carbon monoxide validation over the Arctic during POLARCAT

M. Pommier et al.

[Title Page](#)[Abstract](#)[Introduction](#)[Conclusions](#)[References](#)[Tables](#)[Figures](#)[⏪](#)[⏩](#)[◀](#)[▶](#)[Back](#)[Close](#)[Full Screen / Esc](#)[Printer-friendly Version](#)[Interactive Discussion](#)

difference between the smoothed in situ and IASI varies from 1.1 ppbv to 10.6 ppbv between 8.5 km and 0.5 km, respectively.

In conclusion, the lack of vertical sensitivity and collocation issues were found to be the main detrimental factors for plume detection in the IASI data. In these examples, the DOFS varied with season. It was around 1 in spring with a maximum of sensitivity between 2 and 10 km, and reached 1.7 in summer for the Antonov-30 flight case with a peak of sensitivity at 1 to 8 km, and a second peak at 10–13 km. The limited vertical sensitivity smoothed out most of pollution plumes but the application of the IASI AKs to the in situ measurements improves the agreement. Furthermore, background CO concentrations were well captured by the satellite instrument.

5.3 Statistical comparison for the whole dataset

5.3.1 Comparison by aircraft

All IASI and smoothed in situ profiles were averaged by season and aircraft. Figure 10 shows the comparison between an average of all these observations for the spring campaigns and the Fig. 11 for the summer campaigns, in volume mixing ratio. The number of observations varies according to the aircraft from between 5 and 32 in spring and 8 and 22 in summer. In spring, all mean smoothed in situ profiles are higher than mean IASI profiles above 6 km (generally in the climatology part). Except for the DC-8, where the smoothed in situ CO is always higher than IASI by only a few ppbv (~ 3 – 4 ppbv) and for the P-3B, where both profiles are relatively similar up to 6 km, the difference between both profiles reaches ~ 10 ppbv close to 10 km. In summer, for each aircraft, IASI CO is higher than smoothed in situ CO below 8 km altitude (often the in situ part). This bias is found for all polluted cases. Only with the DC-8 and P-3B, is the smoothed in situ CO higher than IASI CO at each level. Due to the lack of IASI vertical sensitivity in first level, the maximum of difference is found at the surface, 120 ppbv with the P-3B and 20–30 ppbv with the other four aircraft. This seasonal difference close to the surface is correlated to improvement IASI vertical resolution close to the surface

IASI carbon monoxide validation over the Arctic during POLARCAT

M. Pommier et al.

Title Page

Abstract

Introduction

Conclusions

References

Tables

Figures

⏪

⏩

◀

▶

Back

Close

Full Screen / Esc

Printer-friendly Version

Interactive Discussion



in summer. The DOFS varies between 1.0 and 1.10 with a maximum of sensitivity between 2 and 10 km, and in summer between 1.45 and 1.55 with generally peak sensitivity at 2–8 km, and often a second region of enhanced sensitivity at 9–12 km (not shown).

This comparison was also performed for total columns, with mean values summarized in Table 3, for the spring campaigns and Table 4 for the summer campaigns. The mean total columns are in good agreement with a relative difference from –5.19% to 1.36% in spring with the WP-3D and the DC-8, respectively, and in a range of 5–10% in summer. In each case, the smoothed in situ CO total column is lower than IASI CO total column in summer, and for two aircraft (DC-8 and P-3B) in spring. Figure 12 shows the correlation between all CO total column data. In both seasons the minimum correlation coefficient, r , is obtained by the ATR-42, $r \sim 0.15$ in spring and $r \sim 0.26$ in summer. In spring, the correlation coefficient, reaches around 0.74 with the P-3B but with only 5 profiles used and in summer 0.84 with the Falcon-20, using 16 profiles. For the other aircraft, in spring, the coefficient is 0.21 and 0.58 for DC-8 and WP-3D, respectively. And in summer, the coefficient ranges between 0.50 and 0.60 for the other aircraft. The overall correlation in spring is 0.37 and in summer 0.67. Furthermore, when limiting the comparison to partial columns, the correlations are improved in the 0–5 km layer, varying from 0.47 to 0.77 in spring (overall $r \sim 0.59$) and from 0.66 to 0.88 (overall $r \sim 0.79$) in summer (Fig. 12). The correlations with the ATR-42, which only measured up to 6–7 km, are the most improved, giving correlation coefficients of 0.53 in spring and 0.70 in summer, showing the importance of a good climatology to complete the profile.

5.3.2 Impact of surface type

A study was performed to evaluate the impact of surface type on the measured CO. When looking at the seasonal variability of the DOFS we found around 1 in spring, around 1.6 in summer over land and around 1.3 over the ocean. This difference is related to a better thermal contrast in the radiance spectra measurements over land in

IASI carbon monoxide validation over the Arctic during POLARCAT

M. Pommier et al.

Title Page

Abstract

Introduction

Conclusions

References

Tables

Figures



Back

Close

Full Screen / Esc

Printer-friendly Version

Interactive Discussion



summer, where the diurnal surface temperature contrast is more intense than for sea due to the limited heat water capacity (Clerbaux et al., 2009). In spring the maximum of sensitivity is found between 2 and 10 km for all surfaces, in summer there are two peaks, 1–8 km and 8–12 km over the land, 1–3 km and 4–11 km over the sea (not shown).

For this study all the profiles (and corresponding total columns) were averaged according to season, for all aircraft, and then separated by sea and land surface type. During spring campaigns, the same number of observations was performed over the sea and over the land (36 each) whereas in summer more profiles were obtained over the land (68, and 11 over the sea). Moreover, in spring most profiles were over snow or frozen sea. In spring, over both surface types, the maximum difference between smoothed in situ and IASI profiles is close to 10%. In spring, over land (Fig. 13a), IASI is similar or slightly higher than smoothed in situ measurements below 6 km while over the sea (Fig. 13b) it is lower by a few ppbv. In summer, IASI is higher than the smoothed in situ below 8.5 km, over land and sea. The difference gradually varies from 45 ppbv (0.5 km) to 0.7 ppbv (8.5 km) over land (Fig. 13c). Over the sea (Fig. 13d), IASI CO is about 10 ppbv higher than smoothed in situ CO at each level.

When comparing IASI CO total columns and the corresponding smoothed in situ data, a good correlation is found over sea in spring (0.73) and over land in summer (0.69). Less good agreement is found in spring over the land (correlation 0.16) and over the sea in summer (0.33). Whatever the surface type, in spring, the mean IASI total column is lower than the corresponding smoothed in situ total columns and the contrary in summer (Table 5). The comparison of partial columns (0–5 km) still improves the correlations with 0.48 over the land and 0.78 over the sea for spring and with 0.81 over the land and 0.51 over the sea in summer (not shown).

IASI carbon monoxide validation over the Arctic during POLARCAT

M. Pommier et al.

Title Page

Abstract

Introduction

Conclusions

References

Tables

Figures



Back

Close

Full Screen / Esc

Printer-friendly Version

Interactive Discussion



6 Conclusions

This paper reports a detailed comparison of CO profiles obtained by the IASI satellite-borne mission with in situ aircraft measurements collected as part of the POLARCAT project during IPY in spring and summer 2008. Various aircraft campaigns collected data in different parts of the Arctic and over different source regions. In particular, data were collected close to and downwind of boreal forest fire emissions in Siberia and Alaska/Canada. The analysis presented here has shown the capability of IASI to observe long-range transport of CO into the Arctic and its potential to detect the broad vertical structure of plumes, in some cases. Using a collocation criterion of ($\pm 0.2^\circ$; ± 1 h) around the flights, we showed that IASI detected several fire events as well as high CO signatures in the boundary layer due to Siberian forest fires in July 2008. Nevertheless, IASI CO retrievals are affected by the type of underlying surface with the detection of high CO events being less efficient over sea ice and snow.

We also presented a statistical comparison between IASI CO profiles and in situ aircraft profiles completed above flight ceilings with a seasonal and latitudinal ACE-FTS climatology (2004 to 2009) and convolved with the IASI AK (called smoothed in situ profiles). The agreement is good (maximum difference of ~ 10 ppbv in spring), taking into account that the air masses sampled are not exactly the same.

In summer, for each aircraft, the IASI CO was found to be higher than smoothed in situ CO below 8 km altitude, whatever the surface type.

Concerning total columns, mean IASI CO are higher than mean smoothed in situ CO in summer, and for two aircraft (DC-8 and P-3B) in spring. The correlation between IASI and the smoothed in situ CO total columns varies between aircraft from 0.15 to 0.74 in spring and 0.26 to 0.84 in summer. Lowest correlations were obtained for French aircraft for each season, which only flew up to 6–7 km. When averaging all aircraft, the correlation is better (around 0.7) over the sea in spring and over the land in summer.

This validation work will need to be extended to others latitudes using other aircraft data (e.g. the MOZAIC program), and to other species (e.g. ozone) retrieved by IASI.

IASI carbon monoxide validation over the Arctic during POLARCAT

M. Pommier et al.

Title Page

Abstract

Introduction

Conclusions

References

Tables

Figures

⏪

⏩

◀

▶

Back

Close

Full Screen / Esc

Printer-friendly Version

Interactive Discussion



Assimilation of IASI CO in global models can be used to quantify pollution export to the Arctic, the budgets of CO and ozone as well as to better constrain CO sources.

Acknowledgements. M. Pommier is supported by a grant from CNES (Centre national d'Etudes Spatiales) and from NOVELTIS. IASI has been developed and built under the responsibility of the CNES. It is flown onboard the MetOp satellite as part of the Eumetsat Polar system. The IASI L1 data are received through the Eumetcast near real time data distribution service. IASI L1 and L2 data are stored in the Ether French atmospheric database (<http://ether.ipsl.jussieu.fr>). We thank Raphaël Adam de Villiers for his contribution. The research in Belgium was funded by the "Actions de Recherche Concertées" (Communauté Française), the Fonds National de la Recherche Scientifique (FRS-FNRS F.4511.08), the Belgian State Federal Office for Scientific, Technical and Cultural Affairs and the European Space Agency (ESA-Prodex C90-327). POLARCAT-France campaigns was funded by French ANR, CNES, CNRS-INSU (LEFE-CHAT), IPEV and EUFAR. POLARCAT-GACE was funded by DLR. The YAK-AEROSIB campaigns were funded by the CNRS-DRI (France), the French Ministry of Foreign Affairs, CEA (France), RAS (Russia) and RFBR (Russia), and operated in collaboration with IAO-SB-RAS, Tomsk, Russia. The ACE mission is supported primarily by the Canadian Space Agency and some support was provided by the UK Natural Environment Research Council (NERC). The authors are grateful to CNRS-INSU for publication support.



The publication of this article is financed by CNRS-INSU.

IASI carbon monoxide validation over the Arctic during POLARCAT

M. Pommier et al.

Title Page

Abstract

Introduction

Conclusions

References

Tables

Figures

⏪

⏩

◀

▶

Back

Close

Full Screen / Esc

Printer-friendly Version

Interactive Discussion



References

- Adam de Villiers, R., Ancellet, G., Pelon, J., Quennehen, B., Scharwzenboeck, A., Gayet, J. F., and Law, K. S.: Airborne measurements of aerosol optical properties related to early spring transport of mid-latitude sources into the Arctic, *Atmos. Chem. Phys. Discuss.*, 9, 27791–27836, doi:10.5194/acpd-9-27791-2009, 2009.
- Ancellet, G., Leclair de Bellevue, J., Mari, C., Nedelec, P., Kukui, A., Borbon, A., and Perros, P.: Effects of regional-scale and convective transports on tropospheric ozone chemistry revealed by aircraft observations during the wet season of the AMMA campaign, *Atmos. Chem. Phys.*, 9, 383–411, doi:10.5194/acp-9-383-2009, 2009.
- Atlas, E. L., Ridley, B. A., and Cantrell, C. A.: The Tropospheric Ozone Production about the Spring Equinox (TOPSE) Experiment: Introduction, *J. Geophys. Res.*, 108(D4), 8353, doi:10.1029/2002JD003172, 2003.
- Badr, O. and Probert, S. D.: Carbon monoxide concentration in the Earth's atmosphere, *Appl. Energ.*, 50(4), 339–372, 1995.
- Baehr, J., Schlager, H., Ziereis, H., Stock, P., van Velthoven, P., Busen, R., Ström, J., and Schumann U.: Aircraft observations of NO, NO_y, CO, and O₃ in the upper troposphere from 60° N to 60° S – Interhemispheric differences at midlatitudes, *Geophys. Res. Lett.*, 30, 1598, doi:10.1029/2003GL016935, 2003.
- Bernath, P. F., McElroy, C. T., Abrams, M. C., Boone, C. D., Butler, M., Camy-Peyret, C., Carleer, M., Clerbaux, C., Coheur, P.-F., Colin, R., DeCola, P., DeMazière, M., Drummond, J. R., Dufour, D., Evans, W. F. J., Fast, H., Fussen, D., Gilbert, K., Jennings, D. E., Llewellyn, E. J., Lowe, R. P., Mahieu, E., McConnell, J. C., McHugh, M., McLeod, S. D., Michaud, R., Midwinter, C., Nassar, R., Nichitiu, F., Nowlan, C., Rinsland, C. P., Rochon, Y. J., Rowlands, N., Semeniuk, K., Simon, P., Skelton, R., Sloan, J. J., Soucy, M.-A., Strong, K., Tremblay, P., Turnbull, D., Walker, K. A., Walkty, I., Wardle, D. A., Wehrle, V., Zander, R., and Zou, J.: Atmospheric Chemistry Experiment (ACE): Mission overview, *Geophys. Res. Lett.*, 32, L15S01, doi:10.1029/2005GL022386, 2005.
- Boone, C. D., Nassar, R., Walker, K. A., Rochon, Y., McLeod, S. D., Rinsland, C. P., and Bernath, P. F.: Retrievals for the atmospheric chemistry experiment Fourier-transform spectrometer, *Appl. Optics*, 44, 7218–7231, 2005.

IASI carbon monoxide validation over the Arctic during POLARCAT

M. Pommier et al.

Title Page

Abstract

Introduction

Conclusions

References

Tables

Figures

⏪

⏩

◀

▶

Back

Close

Full Screen / Esc

Printer-friendly Version

Interactive Discussion



IASI carbon monoxide validation over the Arctic during POLARCAT

M. Pommier et al.

Title Page

Abstract

Introduction

Conclusions

References

Tables

Figures

⏪

⏩

◀

▶

Back

Close

Full Screen / Esc

Printer-friendly Version

Interactive Discussion



- Boynard, A., Clerbaux, C., Coheur, P.-F., Hurtmans, D., Turquety, S., George, M., Hadji-Lazaro, J., Keim, C., and Meyer-Arneke, J.: Measurements of total and tropospheric ozone from IASI: comparison with correlative satellite, ground-based and ozonesonde observations, *Atmos. Chem. Phys.*, 9, 6255–6271, doi:10.5194/acp-9-6255-2009, 2009.
- 5 Clarisse, L., Coheur, P. F., Prata, A. J., Hurtmans, D., Razavi, A., Phulpin, T., Hadji-Lazaro, J., and Clerbaux, C.: Tracking and quantifying volcanic SO₂ with IASI, the September 2007 eruption at Jebel at Tair, *Atmos. Chem. Phys.*, 8, 7723–7734, doi:10.5194/acp-8-7723-2008, 2008.
- 10 Clerbaux, C., Coheur, P.-F., Hurtmans, D., Barret, B., Carleer, M., Colin, R., Semeniuk, K., McConnell, J. C., Boone, C., and Bernath, P.: Carbon monoxide distribution from the ACE-FTS solar occultation measurements, *Geophys. Res. Lett.*, 32, L16S01, doi:10.1029/2005GL022394, 2005.
- 15 Clerbaux, C., George, M., Turquety, S., Walker, K. A., Barret, B., Bernath, P., Boone, C., Borsdorff, T., Cammas, J. P., Catoire, V., Coffey, M., Coheur, P.-F., Deeter, M., De Mazière, M., Drummond, J., Duchatelet, P., Dupuy, E., de Zafra, R., Eddounia, F., Edwards, D. P., Emmons, L., Funke, B., Gille, J., Griffith, D. W. T., Hannigan, J., Hase, F., Höpfner, M., Jones, N., Kagawa, A., Kasai, Y., Kramer, I., Le Flochmoën, E., Livesey, N. J., López-Puertas, M., Luo, M., Mahieu, E., Murtagh, D., Nédélec, P., Pazmino, A., Pumphrey, H., Ricaud, P., Rinsland, C. P., Robert, C., Schneider, M., Senten, C., Stiller, G., Strandberg, A., Strong, K., Sussmann, R., Thouret, V., Urban, J., and Wiacek, A.: CO measurements from the ACE-FTS satellite instrument: data analysis and validation using ground-based, airborne and spaceborne observations, *Atmos. Chem. Phys.*, 8, 2569–2594, doi:10.5194/acp-8-2569-2008, 2008.
- 20 Clerbaux, C., Boynard, A., Clarisse, L., George, M., Hadji-Lazaro, J., Herbin, H., Hurtmans, D., Pommier, M., Razavi, A., Turquety, S., Wespes, C., and Coheur, P.-F.: Monitoring of atmospheric composition using the thermal infrared IASI/MetOp sounder, *Atmos. Chem. Phys.*, 9, 6041–6054, doi:10.5194/acp-9-6041-2009, 2009.
- 25 Coheur, P.-F., Herbin, H., Clerbaux, C., Hurtmans, D., Wespes, C., Carleer, M., Turquety, S., Rinsland, C. P., Remedios, J., Hauglustaine, D., Boone, C. D., and Bernath, P. F.: ACE-FTS observation of a young biomass burning plume: first reported measurements of C₂H₄, C₃H₆O, H₂CO and PAN by infrared occultation from space, *Atmos. Chem. Phys.*, 7, 5437–5446, doi:10.5194/acp-7-5437-2007, 2007.
- 30

**IASI carbon
monoxide validation
over the Arctic during
POLARCAT**

M. Pommier et al.

Title Page

Abstract

Introduction

Conclusions

References

Tables

Figures

⏪

⏩

◀

▶

Back

Close

Full Screen / Esc

Printer-friendly Version

Interactive Discussion



Coheur, P.-F., Clarisse, L., Turquety, S., Hurtmans, D., and Clerbaux, C.: IASI measurements of reactive trace species in biomass burning plumes, *Atmos. Chem. Phys.*, 9, 5655–5667, doi:10.5194/acp-9-5655-2009, 2009.

5 Fehsenfeld, F. C., Ancellet, G., Bates, T. S., Goldstein, A. H., Hardesty, R. M., Honrath, R., Law, K. S., Lewis, A. C., Leaitch, R., McKeen, S., Meagher, J., Parrish, D. D., Pszenny, A. A. P., Russell, P. B., Schlager, H., Seinfeld, J., Talbot, R., and Zbinden, R.: International Consortium for Atmospheric Research on Transport and Transformation (ICARTT): North America to Europe-Overview of the 2004 summer field study, *J. Geophys. Res.*, 111, D23S01, doi:10.1029/2006JD007829, 2006.

10 Fisher, J. A., Jacob, D. J., Purdy, M. T., Kopacz, M., Le Sager, P., Carouge, C., Holmes, C. D., Yantosca, R. M., Batchelor, R. L., Strong, K., Diskin, G. S., Fuelberg, H. E., Holloway, J. S., Hyer, E. J., McMillan, W. W., Warner, J., Streets, D. G., Zhang, Q., Wang, Y., and Wu, S.: Source attribution and interannual variability of Arctic pollution in spring constrained by aircraft (ARCTAS, ARCPAC) and satellite (AIRS) observations of carbon monoxide, *Atmos. Chem. Phys.*, 10, 977–996, doi:10.5194/acp-10-977-2010, 2010.

15 Fuelberg, H. E., Harrigan, D. L., and Sessions, W.: A meteorological overview of the ARCTAS 2008 mission, *Atmos. Chem. Phys.*, 10, 817–842, doi:10.5194/acp-10-817-2010, 2010.

George, M., Clerbaux, C., Hurtmans, D., Turquety, S., Coheur, P.-F., Pommier, M., Hadji-Lazaro, J., Edwards, D. P., Worden, H., Luo, M., Rinsland, C., and McMillan, W.: Carbon monoxide distributions from the IASI/METOP mission: evaluation with other space-borne remote sensors, *Atmos. Chem. Phys.*, 9, 8317–8330, doi:10.5194/acp-9-8317-2009, 2009.

20 Greenaway, K. R.: Experiences with Arctic flying weather, Royal Meteorological Society Canadian Branch, Toronto, Ontario, Canada, 1950.

Harriss, R. C., Wofsy, S. C., Bartlett, D. S., Shipham, M. C., Jacob, D. J., Hoell Jr., J. M., Bendura, R. J., Drewry, J. W., McNeal, R. J., Navarro, R. L., Gidge, R. N., and Rabine, V. E.: The Arctic Boundary Layer Expedition (ABLE 3A): July–August 1988, *J. Geophys. Res.*, 97(D15), 16383–16394, 1992.

Helmig, D., Oltmans, S. J., Morse, T. O., and Dibb, J. E.: What is causing high ozone at Summit, Greenland? , *Atmos. Environ.*, 41, 5031–5043, 2007.

30 Herbin, H., Hurtmans, D., Clerbaux, C., Clarisse, L., and Coheur, P.-F.: H_2^{16}O and HDO measurements with IASI/MetOp, *Atmos. Chem. Phys.*, 9, 9433–9447, doi:10.5194/acp-9-9433-2009, 2009.

**IASI carbon
monoxide validation
over the Arctic during
POLARCAT**

M. Pommier et al.

[Title Page](#)
[Abstract](#)[Introduction](#)[Conclusions](#)[References](#)[Tables](#)[Figures](#)[⏪](#)[⏩](#)[◀](#)[▶](#)[Back](#)[Close](#)[Full Screen / Esc](#)[Printer-friendly Version](#)[Interactive Discussion](#)

Holloway, J. S., Jakoubek, R., Parrish, D., Gerbig, C., Volz-Thomas, A., Schmitgen, S., Fried, A., Wert, B., Henry, B., and Drummond, J.: Airborne intercomparison of vacuum ultraviolet fluorescence and tunable diode laser absorption measurements of tropospheric carbon monoxide, *J. Geophys. Res.-Atmos.*, 105, 24251–24261, 2000.

5 Hurtmans, D., Clerbaux, C., Coheur, P.-F., et al.: FORLI: A Fast Operational Retrieval on Layers code for IASI, in preparation, 2010.

Jacob, D. J., Crawford, J. H., Maring, H., Clarke, A. D., Dibb, J. E., Ferrare, R. A., Hostetler, C. A., Russell, P. B., Singh, H. B., Thompson, A. M., Shaw, G. E., McCauley, E., Pederson, J. R., and Fisher, J. A.: The ARCTAS aircraft mission: design and execution, *Atmos. Chem. Phys. Discuss.*, 9, 17073–17123, doi:10.5194/acpd-9-17073-2009, 2009.

10 Law, K. S. and Stohl, A.: Arctic Air Pollution: Origins and Impacts, *Science*, 315, 1537–1540, doi:10.1126/science.1137695, 2007.

McMillan, W. W., Warner, J. X., McCourt Comer, M., Maddy, E., Chu, A., Sparling, L., Eloranta, E., Hoff, R., Sachse, G., Barnet, C., Razenkov, I., and Wolf, W.: AIRS views transport from 12 to 22 July 2004 Alaskan/Canadian fires: Correlation of AIRS CO and MODIS AOD with forward trajectories and comparison of AIRS CO retrievals with DC-8 in situ measurements during INTEX-A/ICARTT, *J. Geophys. Res.*, 113, D20301, doi:10.1029/2007JD009711, 2008.

15 Mitchell Jr., J. M.: Visual range in the polar regions with particular reference to the Alaskan Arctic, *J. Atmos. Terr. Phys., Special Suppl.*, Pt. I., 195–211, 1957.

20 Nédélec, P., Cammas, J.-P., Thouret, V., Athier, G., Cousin, J.-M., Legrand, C., Abonnel, C., Lecoeur, F., Cayez, G., and Marizy, C.: An improved infrared carbon monoxide analyser for routine measurements aboard commercial Airbus aircraft: technical validation and first scientific results of the MOZAIC III programme, *Atmos. Chem. Phys.*, 3, 1551–1564, doi:10.5194/acp-3-1551-2003, 2003.

Paris, J.-D., Ciais, P., Nédélec, P., Ramonet, M., Belan, B. D., Arshinov, M. Y., Golitsyn, G. S., Granberg, I., Stohl, A., Cayez, G., Athier, G., Boumard, F., and Cousin, J. M.: The YAK-AEROSIB transcontinental aircraft campaigns: new insights on the transport of CO₂, CO and O₃ across Siberia, *Tellus B*, 60(4), 551–568, 2008.

30 Paris, J.-D., Stohl, A., Nédélec, P., Arshinov, M. Yu., Panchenko, M. V., Shmargunov, V. P., Law, K. S., Belan, B. D., and Ciais, P.: Wildfire smoke in the Siberian Arctic in summer: source characterization and plume evolution from airborne measurements, *Atmos. Chem. Phys.*, 9, 9315–9327, doi:10.5194/acp-9-9315-2009, 2009.

IASI carbon monoxide validation over the Arctic during POLARCAT

M. Pommier et al.

Title Page

Abstract

Introduction

Conclusions

References

Tables

Figures

⏪

⏩

◀

▶

Back

Close

Full Screen / Esc

Printer-friendly Version

Interactive Discussion

- Provençal, R., Gupta, M., Owano, T. G., Baer, D. S., Ricci, K. N., O’Keefe, A., and Podolske, J. R.: Cavity-enhanced quantum-cascade laser-based instrument for carbon monoxide measurements, *Appl. Optics*, 44(31), 6712–6717, 2005.
- Razavi, A., Clerbaux, C., Wespes, C., Clarisse, L., Hurtmans, D., Payan, S., Camy-Peyret, C., and Coheur, P. F.: Characterization of methane retrievals from the IASI space-borne sounder, *Atmos. Chem. Phys.*, 9, 7889–7899, doi:10.5194/acp-9-7889-2009, 2009.
- Rinsland, C. P., Dufour, G., Boone, C. D., Bernath, P. F., Chiou, L., Coheur, P.-F., Turquety, S., and Clerbaux, C.: Satellite boreal measurements over Alaska and Canada during June–July 2004: Simultaneous measurements of upper tropospheric CO, C₂H₆, HCN, CH₃Cl, CH₄, C₂H₂, CH₃OH, HCOOH, OCS, and SF₆ mixing ratios, *Global Biogeochem. Cy.*, 21, GB3008, doi:10.1029/2006GB002795, 2007.
- Rodgers, C. D.: Inverse methods for atmospheric sounding: theory and practice, Ser. Atmos. Ocean. Planet. Phys. 2, World Sci., Hackensack, N. J., 2000.
- Rodgers, C. D. and Connor, B. J.: Intercomparison of remote sounding instruments, *J. Geophys. Res.*, 108(D3), 4116, doi:10.1029/2002JD002299, 2003.
- Sachse, G. W., Hill, G. F., Wade, L. O., and Perry, M. G.: Fast response, high precision carbon monoxide sensor using a tunable diode laser absorption technique, *J. Geophys. Res.*, 92, 2071–2081, 1987.
- Shindell, D., Faluvegi, G., Lacis, A., Hansen, J., Ruedy, R., and Aguilar, E.: Role of tropospheric ozone increases in 20th-century climate change, *J. Geophys. Res.*, 111, D08302, doi:10.1029/2005JD006348, 2006.
- Shindell, D. T., Chin, M., Dentener, F., Doherty, R. M., Faluvegi, G., Fiore, A. M., Hess, P., Koch, D. M., MacKenzie, I. A., Sanderson, M. G., Schultz, M. G., Schulz, M., Stevenson, D. S., Teich, H., Textor, C., Wild, O., Bergmann, D. J., Bey, I., Bian, H., Cuvelier, C., Duncan, B. N., Folberth, G., Horowitz, L. W., Jonson, J., Kaminski, J. W., Marmer, E., Park, R., Pringle, K. J., Schroeder, S., Szopa, S., Takemura, T., Zeng, G., Keating, T. J., and Zuber, A.: A multi-model assessment of pollution transport to the Arctic, *Atmos. Chem. Phys.*, 8, 5353–5372, doi:10.5194/acp-8-5353-2008, 2008.
- Schlüssel, P., Hultberg, T. H., Phillips, P. L., August, T., and Calbet, X.: The operational IASI Level 2 processor, *Adv. Space Res.*, 36, 982, 2005.
- Stohl, A.: Characteristics of atmospheric transport into the Arctic troposphere, *J. Geophys. Res.*, 111, D11306, doi:10.1029/2005JD006888, 2006.

**IASI carbon
monoxide validation
over the Arctic during
POLARCAT**

M. Pommier et al.

Title Page

Abstract

Introduction

Conclusions

References

Tables

Figures

⏪

⏩

◀

▶

Back

Close

Full Screen / Esc

Printer-friendly Version

Interactive Discussion



- Turquety, S., Logan, J. A., Jacob, D. J., Hudman, R. C., Leung, F. Y., Heald, C. L., Yantosca, R. M., Wu, S., Emmons, L. K., Edwards, D. P., and Sachse, G. W.: Inventory of boreal fire emissions for North America in 2004: the importance of peat burning and pyro-convective injection, *J. Geophys. Res.*, 112, D12S03, doi:10.1029/2006JD007281, 2007.
- 5 Turquety, S., Clerbaux, C., Law, K., Coheur, P.-F., Cozic, A., Szopa, S., Hauglustaine, D. A., Hadji-Lazaro, J., Gloudemans, A. M. S., Schrijver, H., Boone, C. D., Bernath, P. F., and Edwards, D. P.: CO emission and export from Asia: an analysis combining complementary satellite measurements (MOPITT, SCIAMACHY and ACE-FTS) with global modeling, *Atmos. Chem. Phys.*, 8, 5187–5204, doi:10.5194/acp-8-5187-2008, 2008.
- 10 Turquety, S., Hurtmans, D., Hadji-Lazaro, J., Coheur, P.-F., Clerbaux, C., Josset, D., and Tsamalis, C.: Tracking the emission and transport of pollution from wildfires using the IASI CO retrievals: analysis of the summer 2007 Greek fires, *Atmos. Chem. Phys.*, 9, 4897–4913, doi:10.5194/acp-9-4897-2009, 2009.
- 15 Wan, Z.: New refinements and validation of the MODIS land-surface temperature/emissivity products, *Remote Sens. Environ.*, 112, 59–74, 2008.
- Warneke, C., Bahreini, R., Brioude, J., Brock, C. A., de Gouw, J. A., Fahey, D. W., Froyd, K. D., Holloway, J. S., Middlebrook, A., Miller, L., Montzka, S., Murphy, D. M., Peischl, J., Ryerson, T. B., Schwarz, J. P., Spackman, J. R., and Veres, P.: Biomass burning in Siberia and Kazakhstan as an important source for haze over the Alaskan Arctic in April 2008, *Geophys. Res. Lett.*, 36, L02813, doi:10.1029/2008GL036194, 2009.
- 20 Wespes, C., Hurtmans, D., Clerbaux, C., Santee, M. L., Martin, R. V., and Coheur, P. F.: Global distributions of nitric acid from IASI/MetOP measurements, *Atmos. Chem. Phys.*, 9, 7949–7962, doi:10.5194/acp-9-7949-2009, 2009.
- Yurganov, L. N., McMillan, W. W., Dzhola, A. V., Grechko, E. I., Jones, N. B., and van der Werf, G. R.: Global AIRS and MOPITT CO measurements: Validation, comparison, and links to biomass burning variations and carbon cycle, *J. Geophys. Res.*, 113, D09301, doi:10.1029/2007JD009229, 2008.

IASI carbon monoxide validation over the Arctic during POLARCAT

M. Pommier et al.

Table 1. Synopsis of CO measurements onboard 6 aircraft involved during ARCTAS (DC-8, P-3B), ARCPAC (WP-3D), POLARCAT (ATR-42, Falcon-20) and YAK-AEROSIB (Antonov-30) campaigns.

Aircraft	Reference	Technique	Averaging time	Accuracy	Precision	Detection limit
DC-8	(Sachse et al., 1987)	TDLAS	1 s	2%	1 ppb	N/A
P-3B	(Provencal et al., 2005)	ICOS	1 s	2%	2 ppb	3 ppb
WP-3D	(Holloway et al., 2000)	VUV fluorescence	1 s	1%	2 ppb	2 ppb
ATR-42	(Nédélec et al., 2003)	IR absorption correlation gas analyser	30 s	5%	5 ppb	10 ppb
Falcon-20	(Baehr et al., 2003)	UV fluorescence	4 s	5%	2 ppb	2 ppb
Antonov-30	(Nédélec et al., 2003; Paris et al., 2008)	IR absorption correlation gas analyser	30 s	5%	5 ppb	10 ppb

Title Page

Abstract

Introduction

Conclusions

References

Tables

Figures

⏪

⏩

◀

▶

Back

Close

Full Screen / Esc

Printer-friendly Version

Interactive Discussion

IASI carbon
monoxide validation
over the Arctic during
POLARCAT

M. Pommier et al.

Title Page

Abstract

Introduction

Conclusions

References

Tables

Figures

◀

▶

◀

▶

Back

Close

Full Screen / Esc

Printer-friendly Version

Interactive Discussion

Table 2. Summary of the performance of the fit in terms of CO total columns, residual RMS, bias and DOFS. For each case, the average and standard deviation over the regions of reference is provided. The regions are defined as: Pacific Ocean (130 180 W; 40 55 N), North America (60 120 W]; 50 70 N), Asia (100 160 E; 50 70 N), Europe (10 W 20 E; 40 60 N), North Pole (180 W 180 E; 75 90 N).

Day		April 2008				July 2008			
		total CO (10^{18} molecules/ cm^2)	RMS ($10^{-9}\text{W}/$ $\text{cm}^2 \text{cm}^{-1} \text{sr}$)	Bias (% RMS)	DOFS	total CO (10^{18} molecules $/\text{cm}^2$)	RMS ($10^{-9}\text{W}/$ $\text{cm}^2 \text{cm}^{-1} \text{sr}$)	Bias (% RMS)	DOFS
Day	Pacific Ocean polluted condition*	2.56±0.26 3.45±0.60	1.46±0.26 1.50±0.34	-5.36±8.17 -8.01±9.04	1.19±0.08 1.16±0.08	2.07±0.33 3.63±0.79	1.52±0.30 1.84±0.76	-4.30±8.28 -11.14±10.70	1.30±0.11 1.17±0.12
	North America polluted condition*	2.29±0.36 3.40±1.04	1.28±0.23 1.67±0.46	-4.52±9.35 -15.35±9.66	1.08±0.11 1.01±0.14	2.09±0.29 3.63±0.98	1.69±0.51 2.21±0.76	-1.41±9.65 -10.82±14.24	1.47±0.16 1.40±0.18
	Asia polluted condition*	2.38±0.31 3.62±1.03	1.25±0.22 1.41±0.39	-4.72±8.73 -7.63±10.53	1.08±0.10 1.05±0.15	2.03±0.35 4.50±1.94	1.70±0.44 1.93±0.68	-1.08±7.95 -3.75±10.27	1.51±0.17 1.40±0.22
	Europe polluted condition*	2.39±0.27 3.28±0.29	1.51±0.32 1.92±0.51	-0.94±8.97 -11.13±7.12	1.31±0.13 1.30±0.13	1.91±0.26 3.28±0.31	1.76±0.47 2.52±0.82	-0.10±7.30 -12.8±4.98	1.57±0.19 1.41±0.15
	North Pole polluted condition*	2.12±0.42 3.37±0.39	1.16±0.14 1.46±0.34	-5.90±7.15 -13.85±8.63	1.00±0.10 0.94±0.11	1.96±0.35 3.40±0.43	1.42±0.33 1.92±0.67	-4.62±10.09 -14.29±13.98	1.50±0.13 1.35±0.13
Night	Pacific Ocean polluted condition*	2.60±0.24 3.47±0.46	1.40±0.28 1.56±0.47	-5.62±7.95 -8.75±8.83	1.22±0.09 1.16±0.09	2.12±0.32 3.65±0.75	1.55±0.39 2.03±1.16	-3.90±8.05 -12.44±13.93	1.33±0.11 1.21±0.13
	North America polluted condition*	2.31±0.35 3.41±0.40	1.24±0.24 1.86±0.53	-5.79±7.07 -17.22±6.54	1.06±0.14 0.99±0.16	2.10 ±0.31 3.77±3.34	1.60±0.46 1.91±0.66	-1.55±7.63 -7.08±10.34	1.37±0.11 1.27±0.13
	Asia polluted condition*	2.32±0.35 3.62±0.69	1.22±0.21 1.50±0.40	-5.66±7.18 -12.12±8.63	1.03±0.13 0.98±0.19	2.09±0.35 4.26±1.64	1.59±0.40 1.96±0.77	-1.61±6.77 -6.24±11.13	1.38±0.11 1.33±0.14
	Europe polluted condition*	2.40±0.26 3.20±0.19	1.46±0.31 1.95±0.43	-2.30±7.52 -13.27±5.09	1.26±0.09 1.22±0.09	1.89±0.29 3.27±0.31	1.62±0.35 2.23±0.64	-0.25±6.53 -10.96±7.42	1.47±0.12 1.31±0.11
	North Pole polluted condition*	2.08±0.45 3.53±0.56	1.13±0.14 1.65±0.49	-7.16±8.66 -18.06±10.01	0.96±0.14 0.85±0.13	- -	- -	- -	- -

* The polluted condition are when columns CO exceeding 3×10^{18} molecules/ cm^2 .

IASI carbon monoxide validation over the Arctic during POLARCAT

M. Pommier et al.

Table 3. Mean of IASI and in situ smoothed CO total column, standard deviation and relative difference calculated as followed: $(((\text{IASI-insitu}) \times 200) / (\text{IASI} + \text{insitu})) \times 100$ for each spring campaign.

CO Total Column (10^{18} molecules/cm ²)	DC-8	P-3B	ATR-42	WP-3D
IASI	2.22±0.32	2.16±0.38	2.45±0.28	2.25±0.30
smoothed in situ*	2.19±0.33	2.15±0.17	2.56±0.19	2.37±0.14
relative difference (%)	1.36	0.46	−4.39	−5.19

* See text for details.

Title Page

Abstract

Introduction

Conclusions

References

Tables

Figures

⏪

⏩

◀

▶

Back

Close

Full Screen / Esc

Printer-friendly Version

Interactive Discussion



IASI carbon monoxide validation over the Arctic during POLARCAT

M. Pommier et al.

[Title Page](#)

[Abstract](#)

[Introduction](#)

[Conclusions](#)

[References](#)

[Tables](#)

[Figures](#)

[⏪](#)

[⏩](#)

[◀](#)

[▶](#)

[Back](#)

[Close](#)

[Full Screen / Esc](#)

[Printer-friendly Version](#)

[Interactive Discussion](#)



Table 4. As Table 3 for each summer campaign.

CO Total Column (10^{18} molecules/cm ²)	DC-8	P-3B	ATR-42	Falcon-20	Antonov-30
IASI	2.15±0.54	2.51±0.74	1.72±0.25	1.88±0.38	1.95±0.33
smoothed in situ*	1.93±0.34	2.26±0.53	1.63±0.26	1.74±0.28	1.82±0.17
relative difference (%)	10.78	10.48	5.37	7.73	6.90

* See text for details.

IASI carbon monoxide validation over the Arctic during POLARCAT

M. Pommier et al.

Table 5. Mean of IASI and in situ smoothed CO total column, standard deviation and relative difference calculated as followed: $[(\text{IASI-in situ}) \times 200] / (\text{IASI} + \text{in situ}) \times 100$; for each season, according to surface type.

CO Total Column (10^{18} molecules/cm ²)	spring		summer	
	land	sea	land	sea
IASI	2.24±0.37	2.31±0.27	2.02±0.52	2.31±0.54
smoothed in situ*	2.26±0.33	2.37±0.23	1.87±0.39	2.04±0.26
relative difference (%)	-0.89	-2.56	7.71	12.41

* See text for details.

Title Page

Abstract

Introduction

Conclusions

References

Tables

Figures

⏪

⏩

◀

▶

Back

Close

Full Screen / Esc

Printer-friendly Version

Interactive Discussion



IASI carbon monoxide validation over the Arctic during POLARCAT

M. Pommier et al.

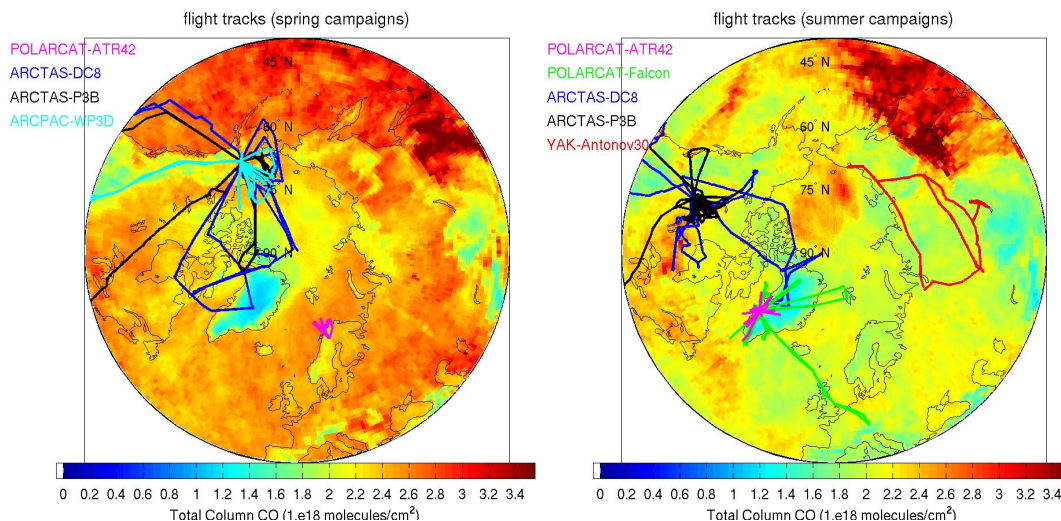


Fig. 1. Overview of all flights of DC-8 (blue), P-3B (black), ATR-42 (magenta), WP-3D (cyan), Falcon (green), Antonov-30 (red) aircraft during the spring (left map) and the summer (right map) campaigns superimposed on IASI CO total column monthly mean map (daytime). The CO data are averaged $1^\circ \times 1^\circ$. The spring map is represented by the April mean and the summer by the July one.

Title Page

Abstract

Introduction

Conclusions

References

Tables

Figures

◀

▶

◀

▶

Back

Close

Full Screen / Esc

Printer-friendly Version

Interactive Discussion

IASI carbon
monoxide validation
over the Arctic during
POLARCAT

M. Pommier et al.

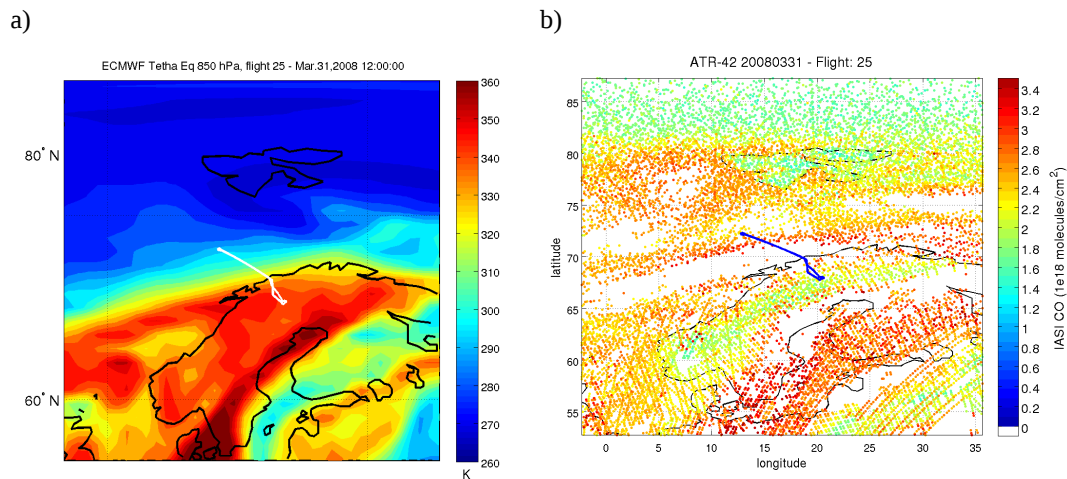


Fig. 2. ECMWF potential equivalent temperature at 850 hPa, above Scandinavia **(a)** and daily IASI CO total column map **(b)** on 31 March 2008. On both maps, ATR-42 flight track is drawn – white line in panel (a) and blue line in panel (b).

[Title Page](#)[Abstract](#)[Introduction](#)[Conclusions](#)[References](#)[Tables](#)[Figures](#)[◀](#)[▶](#)[◀](#)[▶](#)[Back](#)[Close](#)[Full Screen / Esc](#)[Printer-friendly Version](#)[Interactive Discussion](#)

IASI carbon monoxide validation over the Arctic during POLARCAT

M. Pommier et al.

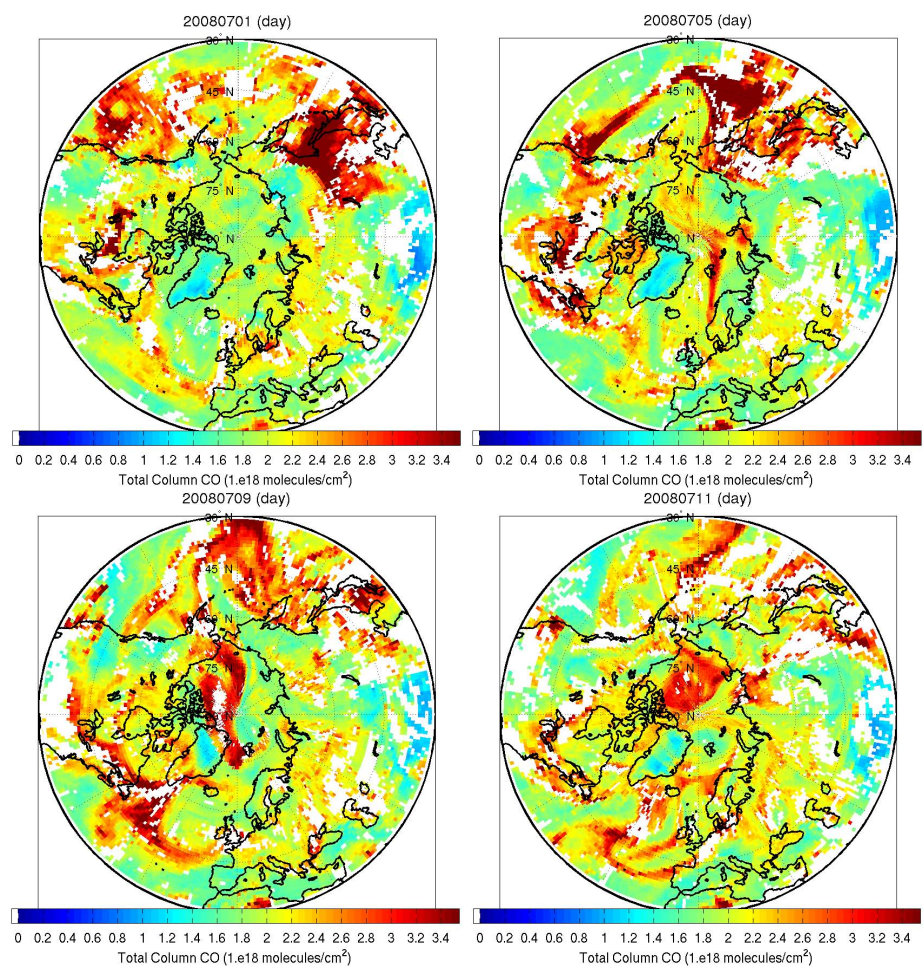


Fig. 3. IASI CO total column daily maps on a 1°×1° grid for the 1, 5, 9 and 11 July 2008.

[Title Page](#)

[Abstract](#) [Introduction](#)

[Conclusions](#) [References](#)

[Tables](#) [Figures](#)

[⏪](#) [⏩](#)

[◀](#) [▶](#)

[Back](#) [Close](#)

[Full Screen / Esc](#)

[Printer-friendly Version](#)

[Interactive Discussion](#)



IASI carbon
monoxide validation
over the Arctic during
POLARCAT

M. Pommier et al.

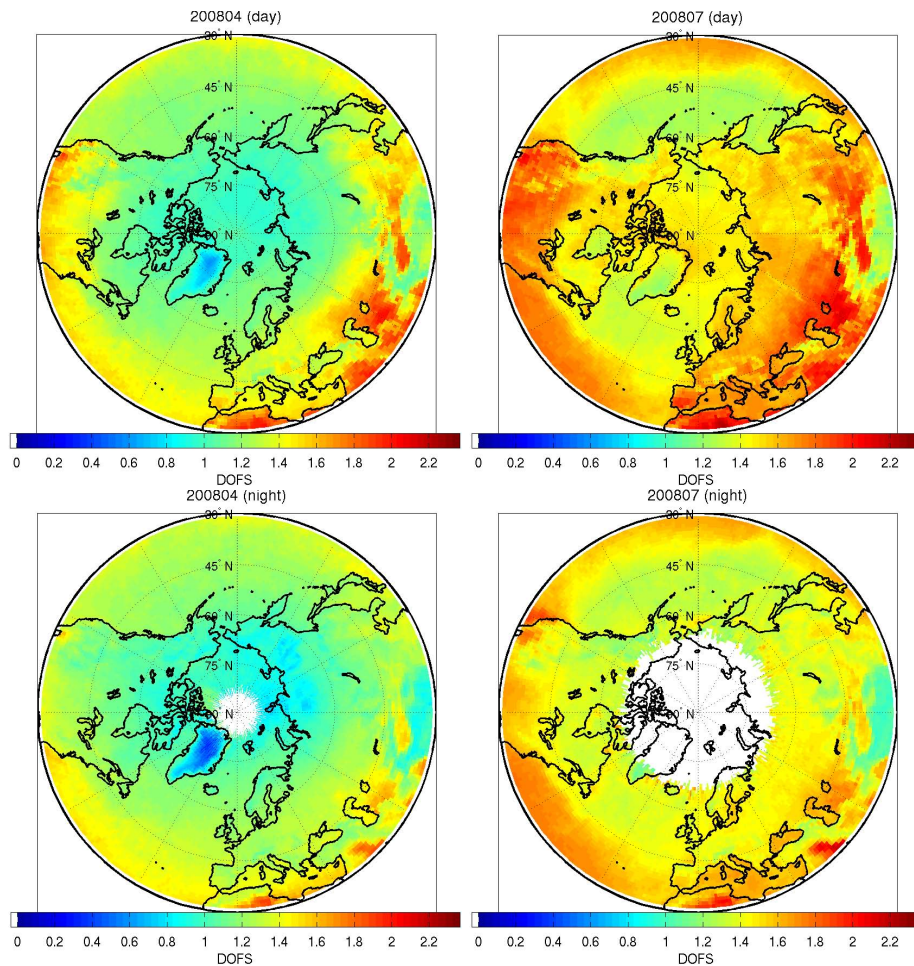


Fig. 4. IASI DOFS monthly maps on a $1^{\circ} \times 1^{\circ}$ grid for April (top panels) and July (bottom panels), for daytime (left) and nighttime (right).

[Title Page](#)[Abstract](#)[Introduction](#)[Conclusions](#)[References](#)[Tables](#)[Figures](#)[◀](#)[▶](#)[◀](#)[▶](#)[Back](#)[Close](#)[Full Screen / Esc](#)[Printer-friendly Version](#)[Interactive Discussion](#)

IASI carbon
monoxide validation
over the Arctic during
POLARCAT

M. Pommier et al.

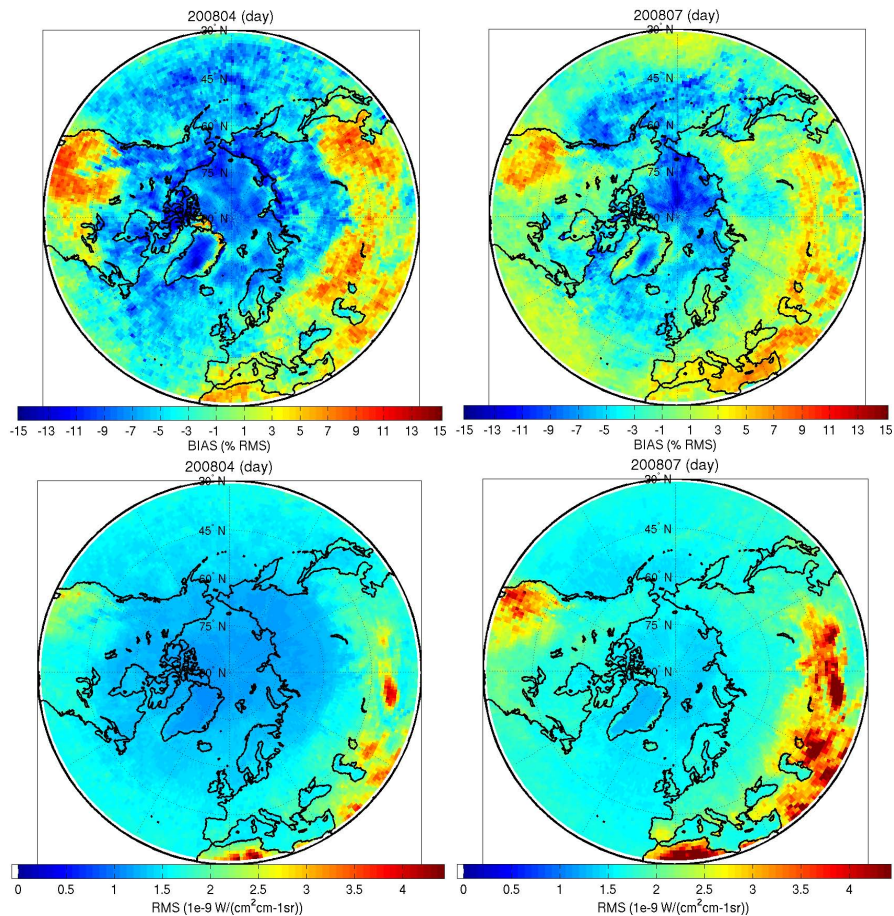


Fig. 5. Maps of IASI daytime RMS error between the observed and the fitted spectrum (left panels), and bias (RMS percentage) (right panels), monthly mean for April 2008 (top) and July 2008 (bottom). Data are on a $1^\circ \times 1^\circ$ grid.

IASI carbon
monoxide validation
over the Arctic during
POLARCAT

M. Pommier et al.

Title Page

Abstract

Introduction

Conclusions

References

Tables

Figures

◀

▶

◀

▶

Back

Close

Full Screen / Esc

Printer-friendly Version

Interactive Discussion

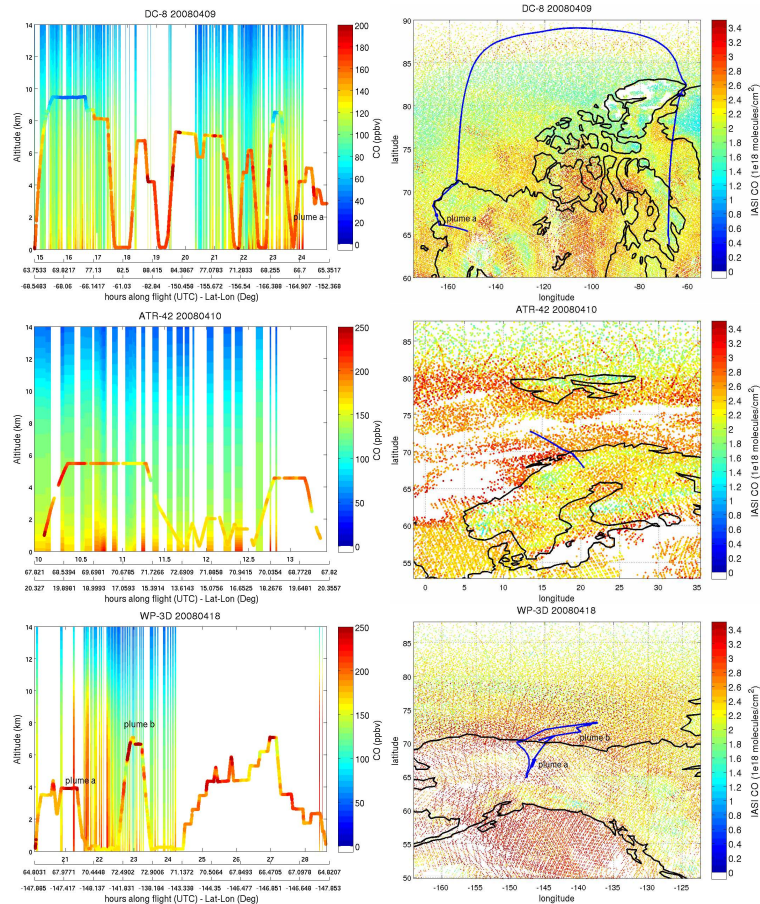


Fig. 6. Left: Cross-sections representing the CO mixing ratio measurements along the DC-8 flight on 9 April (top), the ATR-42 flight on 10 April (middle), and the WP-3D flight on 18 April 2008 (bottom), compared with IASI CO distributions with a criteria of ($\pm 0.2^\circ$; ± 1 h). In situ CO is plotted by altitude versus UTC time along flight, represented by the curve, with latitude and longitude corresponding. Right: maps associated to the cross-sections show the flight track (blue) inside a full day of IASI CO total column observation (coloured dots).

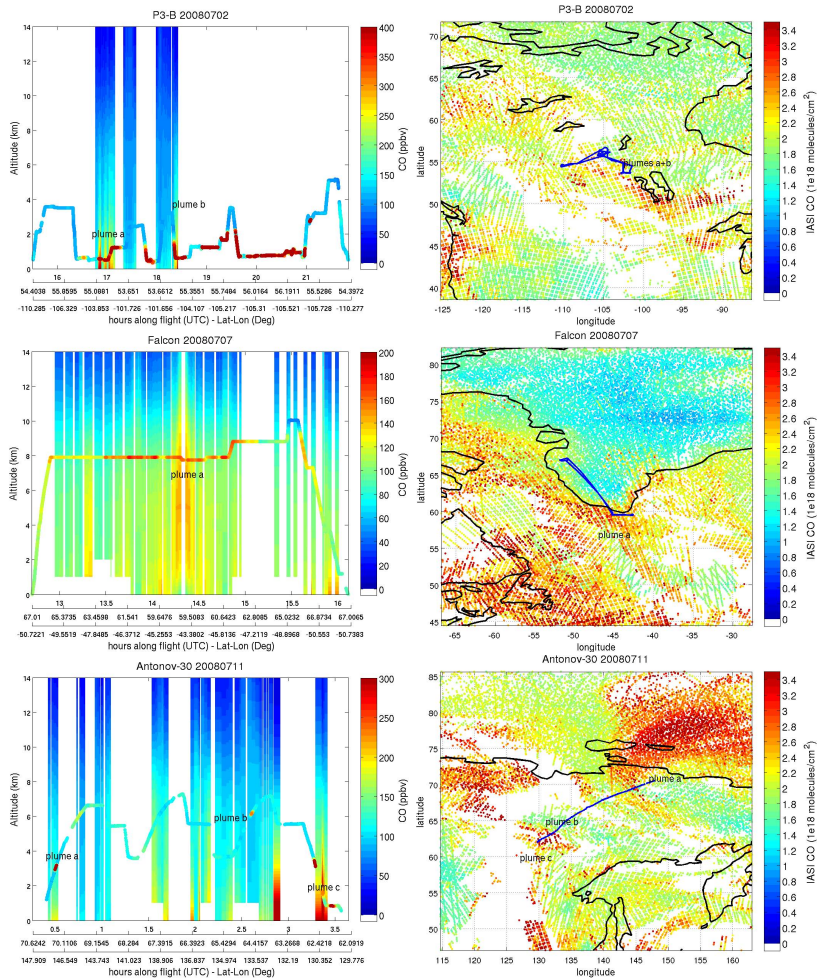


Fig. 7. As Fig. 6 for the P-3B flight on 2 July (top), the Falcon-20 flight on 7 July (middle) and the Antonov-30 flight on 11 July 2008 (bottom).

IASI carbon monoxide validation over the Arctic during POLARCAT

M. Pommier et al.

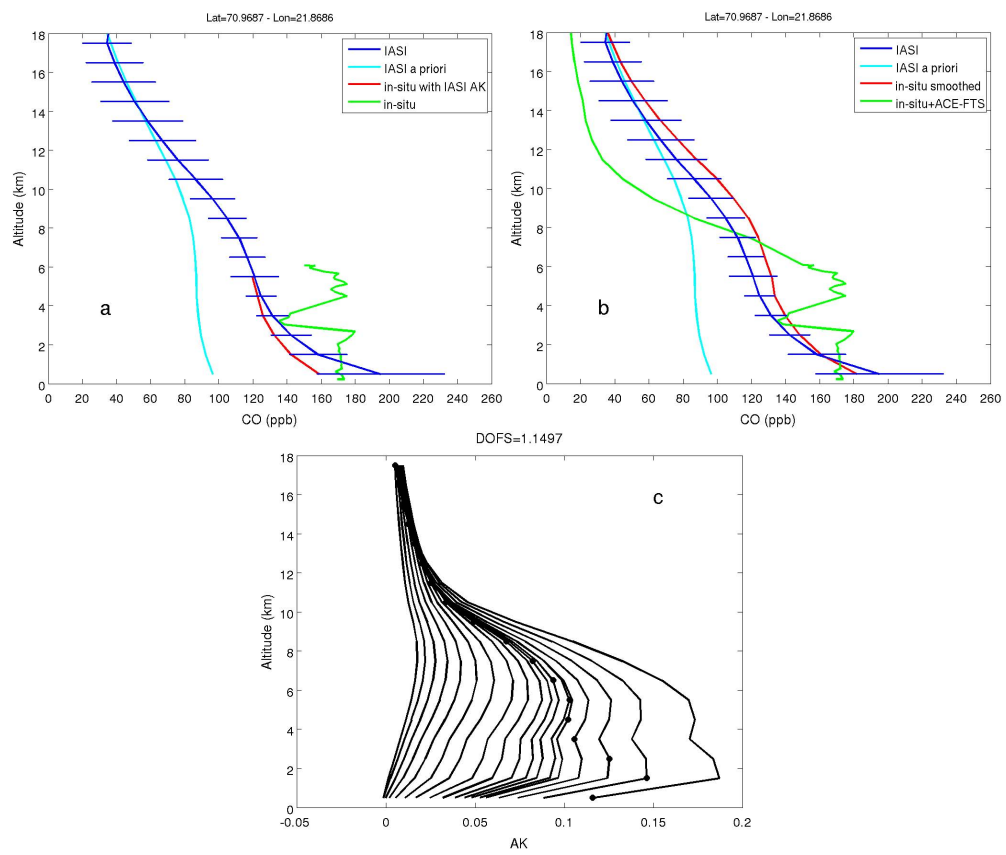


Fig. 8. CO profiles during ATR-42 validation flight on 3 April 2008 around 71° N–22° E. Mixing ratio profiles from IASI (blue) compared with in situ measurements **(a)** and connection to ACE-FTS climatology (green) **(b)**. The cyan line is the IASI a priori and the red line is the in situ smoothed profile. The IASI errors bars correspond to retrievals errors. The IASI averaging kernel is presented in the panel **(c)**. The black points on the averaging kernel show the corresponding altitude.

Title Page

Abstract Introduction

Conclusions References

Tables Figures

◀ ▶

◀ ▶

Back Close

Full Screen / Esc

Printer-friendly Version

Interactive Discussion



IASI carbon
monoxide validation
over the Arctic during
POLARCAT

M. Pommier et al.

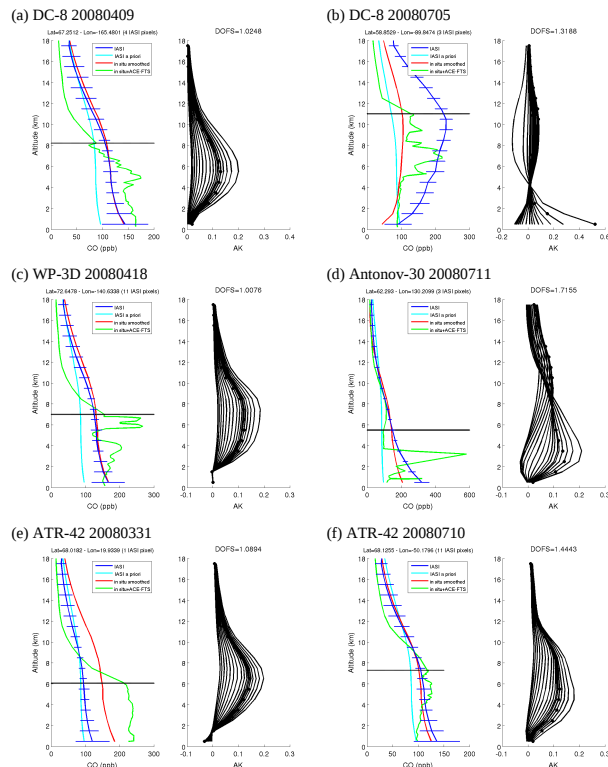


Fig. 9. CO profiles in VMR of IASI (blue) and in situ measurements connected with ACE-FTS climatology (green) and convolved with IASI AK (red) for three examples in spring **(a)-(c)-(e)** and three examples in summer **(b)-(d)-(f)**. The cyan line is the IASI a priori. For each example, the IASI AK is presented in black beside the measurements. The black points on the averaging kernel show the altitude corresponding. The IASI errors bars correspond to retrievals errors. The horizontal black line represents the upper limit of in situ profile. In situ profiles were measured from the DC-8 in 9 April (a) and in 5 July (b), the WP-3D on 18 April (c), the Antonov-30 on 11 July (d), and the ATR-42 on 31 March (e) and on 10 July 2008 (f).

IASI carbon monoxide validation over the Arctic during POLARCAT

M. Pommier et al.

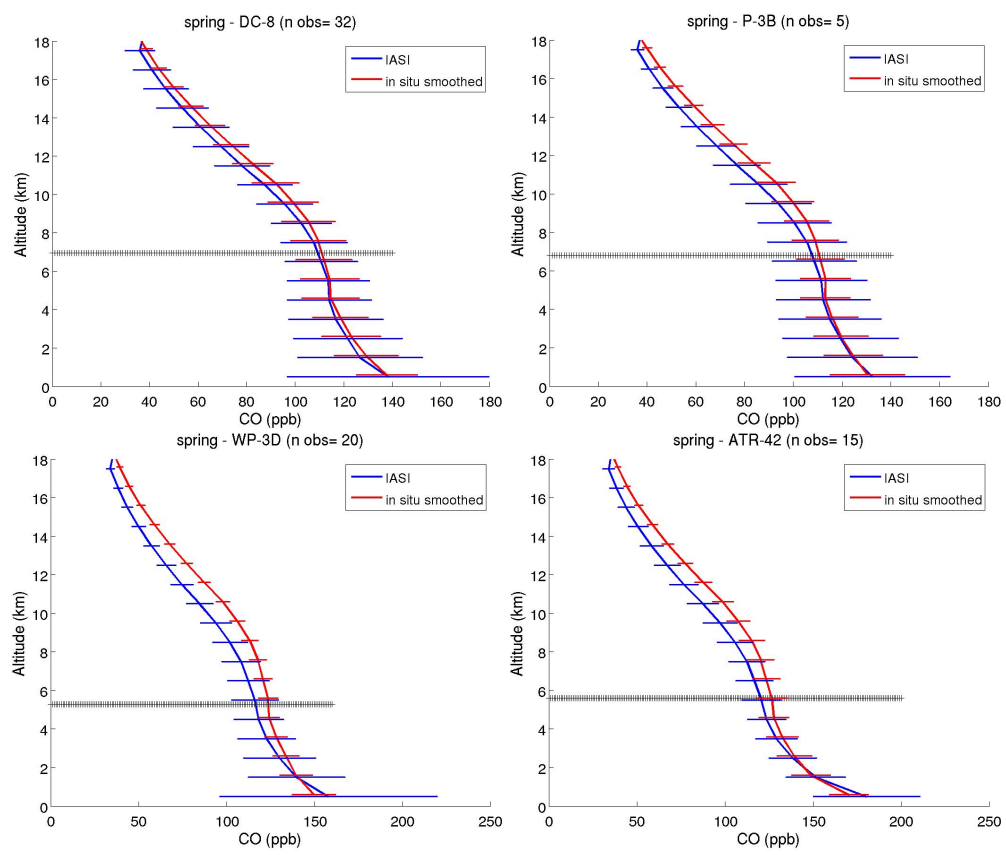


Fig. 10. Summary of mean IASI CO profiles (blue line) and smoothed in situ profiles (red line) in VMR for each aircraft of spring campaigns. The smoothed in situ profiles represent the in situ measurements connected to ACE-FTS climatology and convolved with IASI AK (see text for details). The horizontal black line represents the mean position of the upper limit of in situ profiles. Errors bars represent the variability of measurements.

Title Page	
Abstract	Introduction
Conclusions	References
Tables	Figures
◀	▶
◀	▶
Back	Close
Full Screen / Esc	
Printer-friendly Version	
Interactive Discussion	



IASI carbon monoxide validation over the Arctic during POLARCAT

M. Pommier et al.

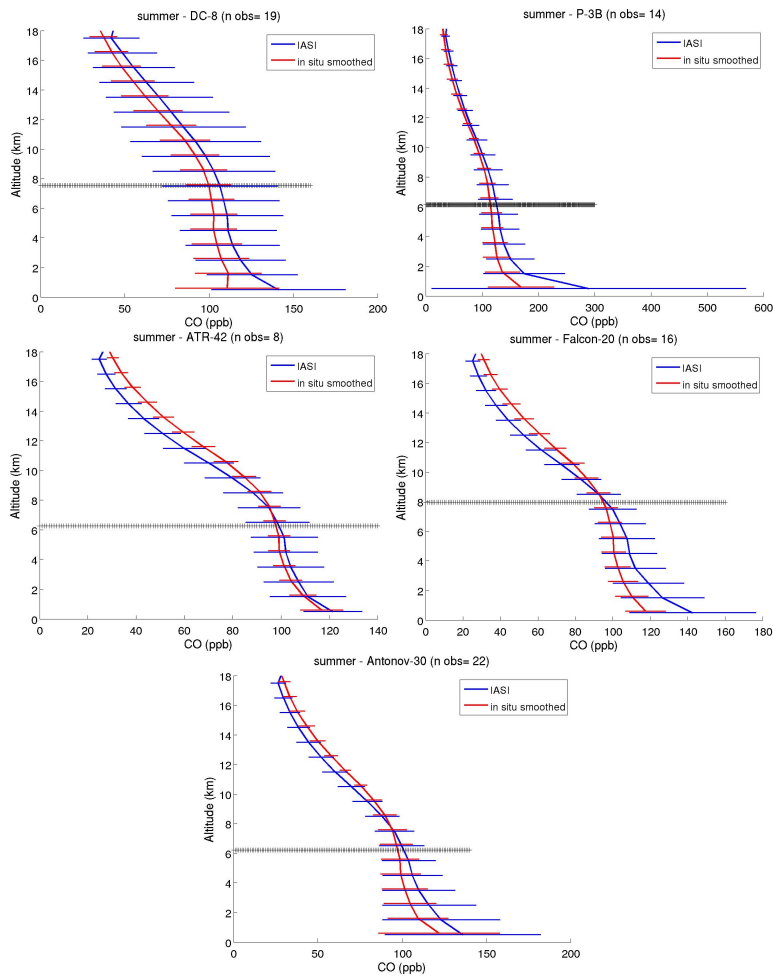


Fig. 11. As Fig. 10 for summer campaigns.

Title Page

Abstract Introduction

Conclusions References

Tables Figures

⏪ ⏩

◀ ▶

Back Close

Full Screen / Esc

Printer-friendly Version

Interactive Discussion



IASI carbon monoxide validation over the Arctic during POLARCAT

M. Pommier et al.

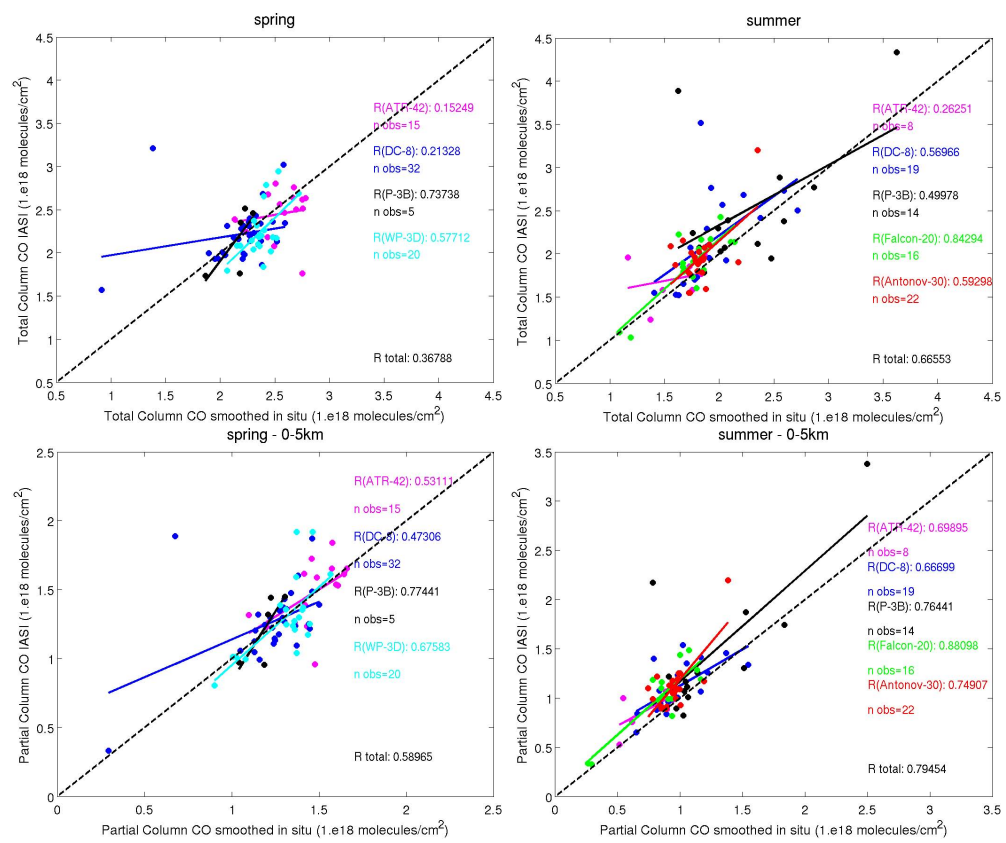


Fig. 12. Scatter plots of the IASI and smoothed in situ CO total columns (top) and 0–5 km partial columns (bottom) for the spring (left panel) and the summer (right panel) campaigns. The coloured lines represent the linear regression between data points for each aircraft: ATR-42 (magenta), DC-8 (blue), P-3B (black), WP-3D (cyan), Falcon-20 (green), and Antonov-30 (red). The black dotted line, of unity slope, is shown for reference.

Title Page

Abstract	Introduction
Conclusions	References
Tables	Figures

⏪
⏩
⏴
⏵

Back	Close
------	-------

Full Screen / Esc

Printer-friendly Version

Interactive Discussion



IASI carbon monoxide validation over the Arctic during POLARCAT

M. Pommier et al.

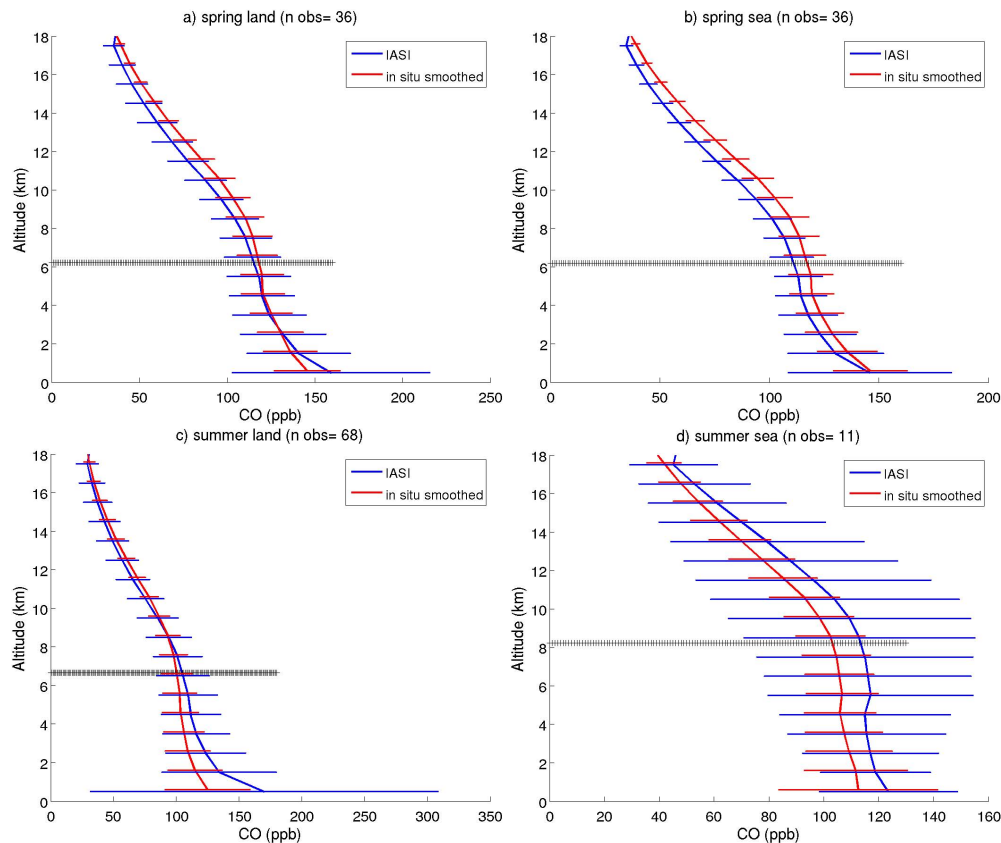


Fig. 13. Summary of mean IASI CO profiles (blue line) and smoothed in situ profiles (red line) in VMR for each season (spring in top panels and summer in bottom panels), over different surfaces (land on the left and sea on the right). The horizontal black line represents the mean position of the upper limit of in situ profiles. Errors bars represent the variability of measurements.

Title Page	
Abstract	Introduction
Conclusions	References
Tables	Figures
◀	▶
◀	▶
Back	Close
Full Screen / Esc	
Printer-friendly Version	
Interactive Discussion	